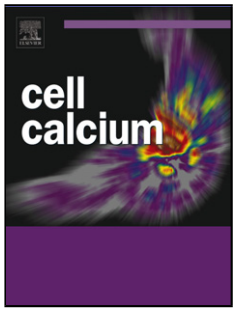

Title: Potent functional uncoupling between STIM1 and Orai1 by dimeric 2-aminodiphenyl borinate analogs

Author: Eunan Hendron Xizhuo Wang Yandong Zhou Xiangyu Cai Jun-Ichi Goto Katsuhiko Mikoshiba Yoshihiro Baba Tomohiro Kurosaki Youjun Wang Donald L. Gill

PII: S0143-4160(14)00160-2
DOI: http://dx.doi.org/doi:10.1016/j.ceca.2014.10.005
Reference: YCECA 1613

To appear in: *Cell Calcium*

Received date: 10-9-2014
Revised date: 10-10-2014
Accepted date: 14-10-2014

Please cite this article as: E. Hendron, X. Wang, Y. Zhou, X. Cai, J.-I. Goto, K. Mikoshiba, Y. Baba, T. Kurosaki, Y. Wang, D.L. Gill, Potent functional uncoupling between STIM1 and Orai1 by dimeric 2-aminodiphenyl borinate analogs, *Cell Calcium* (2014), http://dx.doi.org/10.1016/j.ceca.2014.10.005

*Graphical Abstract

Graphical Abstract

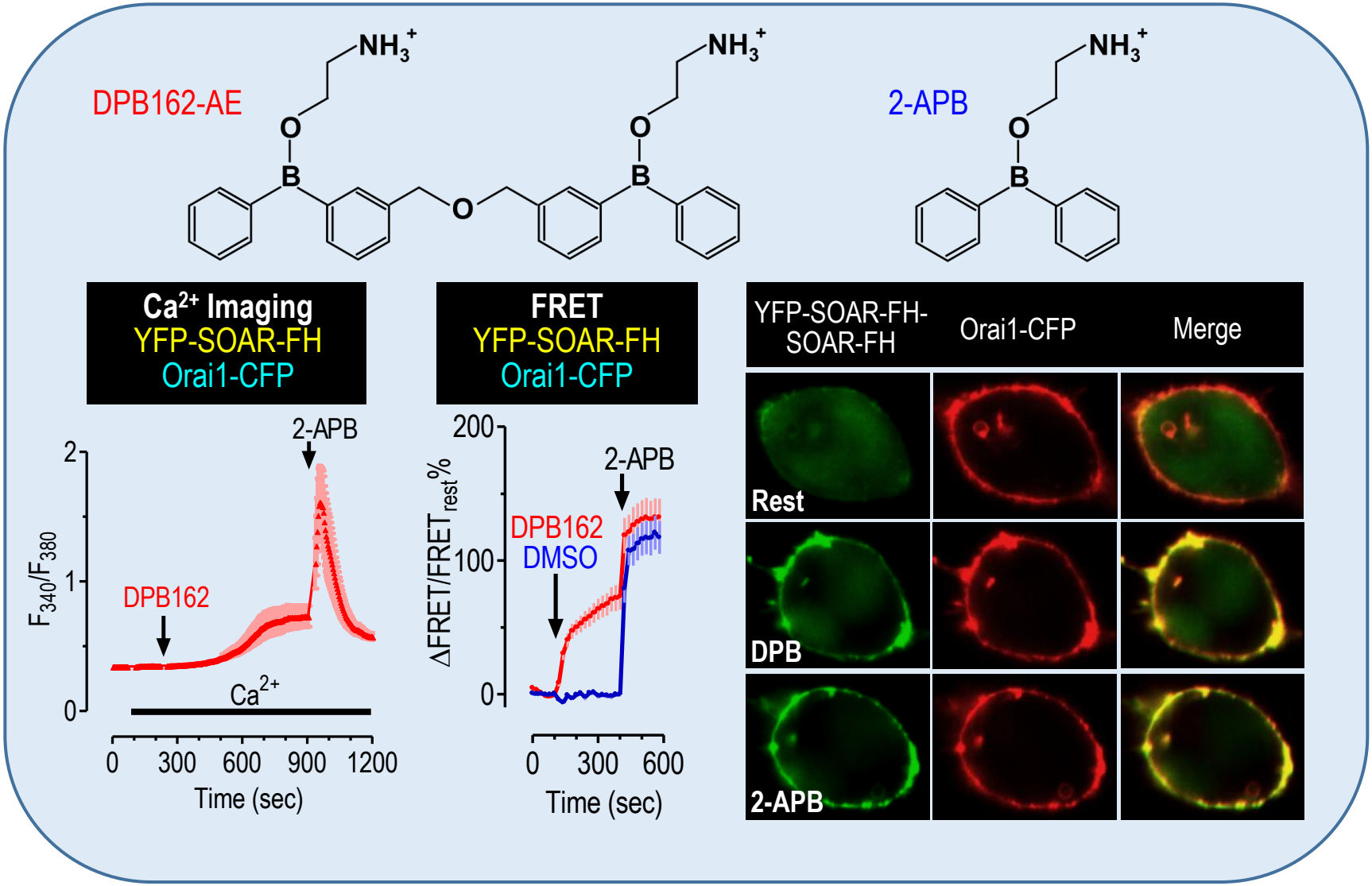

Highlights

- DPB162-AE potently blocks functional coupling between STIM1 and Orai1
- DPB162-AE specifically blocks Orai channel activation and not L-type or TRPC channels
- SOAR-F394H binding to Orai1 is rapidly restored by DPB162-AE
- Coupling of SOAR-F394H to activate Orai1 channels is slow
- The site of action of DPB162-AE is at the STIM1-Orai1 coupling interface

Submitted to Cell Calcium, September 10, 2014
Revised Submission, October 10, 2014

Potent functional uncoupling between STIM1 and Orai1 by dimeric 2-aminodiphenyl borinate analogs

Eunan Hendron[1*], Xizhuo Wang[1,2*], Yandong Zhou[2], Xiangyu Cai[2], Jun-Ichi Goto[3], Katsuhiko Mikoshiba[4], Yoshihiro Baba[5], Tomohiro Kurosaki[5], Youjun Wang[6], and Donald L. Gill[2]

[1] Department of Biochemistry, Temple University School of Medicine, Philadelphia, PA 19140

[2] Department of Cellular and Molecular Physiology
The Pennsylvania State University College of Medicine, Hershey PA 17033

[3] Department of Physiology, Yamagata University School of Medicine, Yamagata 990-9585, Japan

[4] Laboratory for Developmental Neurobiology, RIKEN Brain Science Institute, Saitama 351-0198 Japan

[5] Laboratory for Lymphocyte Differentiation, WPI Immunology Frontier Research Center, Osaka University, Suita, Osaka 565-0871, Japan, and Laboratory for Lymphocyte Differentiation, RIKEN Center for Integrative Medical Sciences, Yokohama, Kanagawa 230-0045, Japan

[6] Beijing Key Laboratory of Gene Resources and Molecular Development
College of Life Sciences, Beijing Normal University, Beijing 100875, P.R. China

*These authors contributed equally to this work

Correspondence should be addressed to:

Donald L. Gill (email: dongill@psu.edu) or Youjun Wang (email: wyoujun@bnu.edu.cn)

ABSTRACT

The coupling of ER Ca^{2+}-sensing STIM proteins and PM Orai Ca^{2+} entry channels generates "store-operated" Ca^{2+} signals crucial in controlling responses in many cell types. The dimeric derivative of 2-aminoethoxydiphenyl borinate (2-APB), DPB162-AE, blocks functional coupling between STIM1 and Orai1 with an IC_{50} (200 nM) 100-fold lower than 2-APB. Unlike 2-APB, DPB162-AE does not affect L-type or TRPC channels or Ca^{2+} pumps at maximal STIM1-Orai1 blocking levels. DPB162-AE blocks STIM1-induced Orai1 or Orai2, but does not block Orai3 or STIM2-mediated effects. We narrowed the DPB162-AE site of action to the STIM-Orai activating region (SOAR) of STIM1. DPB162-AE does not prevent the SOAR-Orai1 interaction but potently blocks SOAR-mediated Orai1 channel activation, yet its action is not as an Orai1 channel pore blocker. Using the SOAR-F394H mutant which prevents both physical and functional coupling to Orai1, we reveal DPB162-AE rapidly restores SOAR-Orai binding but only slowly restores Orai1 channel-mediated Ca^{2+} entry. With the same SOAR mutant, 2-APB induces rapid physical and functional coupling to Orai1, but channel activation is transient. We infer that the actions of both 2-APB and DPB162-AE are directed toward the STIM1-Orai1 coupling interface. Compared to 2-APB, DPB162-AE is a much more potent and specific STIM1/Orai1 functional uncoupler. DPB162-AE provides an important pharmacological tool and a useful mechanistic probe for the function and coupling between STIM1 and Orai1 channels.

Keywords

Calcium, STIM1, STIM2, Orai1, Orai2, Orai3, 2-APB

1. Introduction

Ca^{2+} signals in cells are generated through the function of Ca^{2+} channels that either release stored Ca^{2+} from the endoplasmic reticulum (ER) or allow external Ca^{2+} to enter across the plasma membrane (PM). The ER membrane-spanning STIM proteins are sensors of Ca^{2+} stored in the ER and in response to Ca^{2+} store-depletion trigger the opening of Orai Ca^{2+} entry channels [1]. Decreased ER luminal Ca^{2+} triggers STIM1 activation and translocation into ER-PM junctions where it binds to and opens the highly Ca^{2+}-selective Orai family of "store-operated" PM channels [1, 2]. The store-operated Ca^{2+} entry (SOCE) mediated by Orai channels is important for sustaining Ca^{2+} oscillations, maintaining Ca^{2+} homeostasis, and generating longer-term Ca^{2+} signals that regulate gene expression and cell growth [1, 3]. Changes in the operation of STIM-mediated Orai channel function have important consequences in autoimmunity, inflammation, vascular diseases and cancer [4-6].

The function and control of STIM and Orai proteins has been intensely studied [1, 2, 4, 7]. The luminal N-terminal domain of STIM1 contains EF-hands which sense depletion of Ca^{2+} within the ER [8, 9]. Structural changes in the STIM1 N-terminus triggered by Ca^{2+} dissociation, induce self-association between STIM1 proteins and an important conformational change in the cytoplasmic C-terminus of STIM1 which undergoes unfolding and exposure of the cytoplasmic Orai-interacting site [1, 2, 4]. A short 100-amino acid segment known as the STIM-Orai activating region (SOAR) [10] or CRAC activation domain (CAD) [11] was revealed within the cytoplasmic domain of STIM1 to be the minimal sequence able to both interact with and activate Orai channels. Structural analysis shows SOAR comprises four well-organized helices and exists as a dimer [12]. Biochemical evidence suggests the STIM1 molecule itself is a dimer in its resting and active state [12-15]. The Orai channel protein has four transmembrane helices and crystallography reveals the channel to be a hexamer [16]. The N-terminal helices of each of the six Orai subunits form the central Orai channel pore [17-20]. The Orai1 cytoplasmic N- and C-termini extend into the cytosol in close proximity to each other [16, 21]. It appears that these N- and C-terminal helices of Orai1 combine to interact with STIM1 [11, 22], and both are required for STIM1-induced activation of the Orai channel [22-28].

Although structural and biochemical approaches provide a significant understanding of the molecular interactions between STIM and Orai proteins, pharmacological approaches have not been forthcoming. Thus, there have been few specific chemical modifiers that are useful as probes to examine the STIM-Orai coupling and activation process. One molecule that has been useful is 2-aminoethoxy-diphenyl borinate (2-APB). 2-APB has a complex, biphasic effect on STIM1-induced Orai1 channel

activation, lower levels (1-10 μM) enhancing and higher levels (10-100 μM) strongly inhibiting SOCE mediated by Orai [29, 30]. With sensitivity in the micromolar range, it would not be expected that the actions of 2-APB would be highly specific for Orai channels. Indeed, although widely used as an inhibitor of SOCE, 2-APB has similar inhibitory actions on $InsP_3$ receptor Ca^{2+} release channels [31-33], a range of TRP channels [34-39], and even Ca^{2+} pumps [40, 41]. Despite these other effects, the actions of 2-APB on STIM/Orai-mediated SOCE have some curious and interesting facets. The Orai3 channel is shown to be directly activated by 2-APB without any requirement for STIM proteins [42-46]. 2-APB also has profound actions in promoting the functional coupling between STIM1 with Orai1 [46, 47]. Thus, using certain derivatives or mutants of STIM1 that are unable to bind to Orai1, 2-APB overcomes these defects and induces strong STIM1 binding and Orai1 channel activation [46, 47].

Based on an earlier screen of compounds related to 2-APB [48], two dimeric 2-APB derivatives, DPB162-AE and DPB163-AE (herein referred to as DPB162 and DPB163), were identified with more potent actions on STIM-induced Orai channel activation [33]. Here, we reveal that these compounds have not only high potency but also considerable specificity of action on STIM1/Orai1-dependent SOCE. We narrowed their site of action to modification of the functional coupling between the SOAR fragment of STIM1 and the Orai1 channel. While they have no effect on SOAR-Orai1 interaction, they potently block SOAR-mediated Orai1 channel activation. However, their action is not consistent with modifying the Orai1 channel pore. Using a recently defined point mutation in SOAR (F394H) which completely prevents STIM1-Orai1 coupling [47], we reveal DPB162 can restore binding and permit sustained functional coupling to activate Orai1. With the same SOAR mutant, 2-APB induces a similar but more rapid functional coupling to Orai1, but Orai1 activation is transient. We infer that the actions of both 2-APB and DPB162 are directed toward the STIM1-Orai1 coupling interface. Compared to 2-APB, DPB162 is a much more potent and specific STIM1/Orai1 *functional uncoupler*. But the action of both molecules appears highly dependent on the configuration of the STIM-Orai interface. The mixed activation and inhibition profiles of both molecules likely reflect a fine line between enhancing as opposed to preventing successful coupling of STIM1 to the Orai1 channel.

2. Methods

2.1. Materials and DNA constructs

DPB162 and DPB163 were generously provided by Dr. Katsuhiko Mikoshiba (RIKEN, Japan). EGTA, DMSO, nimodipine and 1-Oleoyl-2-acetyl-*sn*-glycerol (OAG) were purchased from Sigma-Aldrich. Thapsigargin (TG) was from EMD Biosciences (San Diego, CA). 2-APB was from Tocris Bioscience. Fura-2/AM was from Molecular Probes. cDNA for CFP-tagged Orai3 was from James Putney Jr. (NIEHS, Triangle Park, NC), the GFP-α1C plasmid was from Dr. Kurt Beam (Univ. Colorado, Denver CO); TRPC3 cDNA was from Dr. Craig Montell (Johns Hopkins Univ.), TRPC6 cDNA was from BD Biosciences (Mountain View, CA) and subcloned into psDNA3 (Stratagene, La Jolla, CA). STIMct C-terminally YFP-labeled constructs were inserted within the pIRESneo3 plasmid (Clontech, Palo Alto, CA) as described [46, 47]. STIM1ct-4EA-YFP was mutated from STIM1ct-YFP construct, and STIM1-F394H-YFP was mutated from STIM1-YFP. The SOAR sequence was inserted within the pEYFP-c1/pECFP-c1 plasmid (Clontech, Palo Alto, CA) between XhoI/EcoRI sites to create N-terminally-labeled SOAR derivatives. YFP-SOAR-F394H was mutated from YFP-SOAR. A repeated SOAR sequence was inserted at the end of YFP-SOAR with a 72 bp linker GGCGGCTCTGGAGG-TAGCGGAGGTGGAATTCTGCAGTCGAGGGGTGGATCCGGTGGGTCCGGCGGATCCGGC (translated as 24 amino acids GGSGGSGGGILQSRGGSGGSGGSG) to make the YFP-SOAR-SOAR construct. YFP-SOAR-F394H-SOAR-F394H was mutated from YFP-SOAR-SOAR. The constructs YFP-SOAR-F394H, YFP-SOAR-SOAR, YFP-SOAR-F394H-SOAR-F394H, SOAR-F394H were made by Mutagenex, NJ.

2.2. Cell culture and transfection

HEK293 stably-transfected cells were derived and maintained in Dulbecco's modified Eagle's medium (Mediatech Inc, Manassas, VA) supplemented with 10% fetal bovine serum, penicillin and streptomycin (Gemini Bioproducts, CA) at 37 °C with 5% CO2 in G418 (100 μg/ml) as previously described [49, 50]. DT40 cells were maintained in RPMI 1640 (Mediatech Inc, Manassas, VA) as described [30]. Rat basophilic leukemia cell line RBL-2H3 were grown in the same medium but with heat-inactivated serum [51, 52]. Jurkat and CEM.3-71 cells were from ATCC (Rockville, MD). All plasmid transfections were undertaken by electroporation using the Bio-Rad Gene Pulser Xcell system in OPTI-MEM medium as previously described [47]. DNA constructs were introduced by electroporation at 180 V, 25ms in 4 mm cuvettes (Molecular BioProducts). Transfected cells were cultured on cover slips (25mm) in OPTI-MEM with 5% FBS and measurements undertaken 14-24 hours after transfection as

previously described [47, 53]. HEK293 cells stably expressing Orai1-CFP (HEK-Orai cells) or Orai3-CFP were generated by electroporation of pIRES constructs and selection as described [49]. Transient transfection levels of STIM1, STIM1-F394H, STIM1ct, and SOAR constructs were quantified previously [46, 47, 54]. We noted that transient transfection of the YFP-SOAR-F394H mutant resulted in expression in HEK-Orai1 cells that was lower than expression of the wildtype YFP-SOAR (Fig. S1A). However, the proportion of cells that were expressing the YFP-SOAR-F394H mutant (93 out of 655 cells; 14%) was substantially below that of YFP-SOAR-expressing cells (220 out of 393; 56%). Indeed, the YFP-intensity per cell for these two populations were not so different as shown in Fig. S1B. As noted below, transfection with the dimeric YFP-SOAR-SOAR and YFP-SOAR-F394H-SOAR-F394H constructs, was more consistent with approximately 50% of cells transfected and with very similar levels of YFP-intensity per cell. Transfection of SOAR mutants The Orai1, Orai2, STIM1 and STIM2 knockout DT40 cell lines were generous gifts from Dr. Tomohiro Kurosaki (RIKEN, Japan). STIM or Orai knockout DT40 cells were generated as described by Baba et al. [55]http://www.pnas.org/content/106/18/7391.full - ref-37.

2.3. Cytosolic Ca^{2+} measurements

Intracellular Ca^{2+} levels were measured by ratiometric imaging using fura-2. Loading of fura-2 and imaging of fura-2 fluorescence as described previously [56] utilized loading and fluorescence solutions comprising: 107 mM NaCl, 7.2 mM KCl, 1.2 mM $MgCl_2$, 11.5 mM glucose, 20 mM Hepes-NaOH, pH 7.2. During dye-loading, cells were treated with 2 μM fura-2/AM for 30 min at room temperature, then transferred to fura-2-free solution for a further 30 min. Ratio fluorescence imaging was measured utilizing the Leica DMI 6000B fluorescence microscope controlled by Slidebook 5.0 software (Intelligent Imaging Innovations; Denver, CO). Consecutive excitation at 340nm (F_{340}) and 380nm light (F_{380}) was undertaken every two seconds; emission fluorescence was collected at 505 nm. Intracellular Ca^{2+} levels are shown as F_{340}/F_{380} ratios obtained from groups of 5-35 single cells on coverslips. All Ca^{2+} imaging experiments were performed at room temperature and representative traces of at least three independent repeats are shown as mean ± SEM.

2.4. Automated multi-well Ca^{2+} measurements

DT40 cells were cultured as previously described [46]. Prior to plating, cells were loaded in 15 ml tubes with fluo-4 while in suspension, as described for fura-2. Following fluo-4 loading, cells were counted in a Bio-Rad Automated Cell Counter and re-suspended in 3 mM Ca^{2+} imaging buffer, to provide a final cell density of 55,000 cells per well in the 384 well plate. 20 μl of re-suspended cells were plated in each well in 384-well poly-*l*-lysine coated plates. Plates was centrifuged (3,000 rpm, 5 min) to settle

cells on the bottom. Plates were then transferred to the Hamamatsu μCell Functional Drug Screening System. For each experiment, two compound-addition plates were prepared for automatic loading and solution change by the imaging system. The first plate contained all applicable drugs (TG; DPBs) at 6x desired final concentration, 20 μl per well. The automatic solution change added 4 μl of each solution to the cell plate with 20 μl measuring solution, establishing the final concentration of 2 μM for TG or DPBs at the concentrations shown. For the second plate, 3 mM Ca^{2+} imaging buffer was added at 5x.

2.5. Förster resonance energy transfer (FRET) measurements

These measurements were as described previously [47]. To determine FRET signals between stably expressed Orai1-CFP and transiently expressed YFP-tagged STIM fragments, we used the Leica DMI 6000B fluorescence microscope equipped with CFP ($438_{Ex}/483_{Em}$), YFP ($500_{Ex}/542_{Em}$), $FRET_{raw}$ ($438_{Ex}/542_{Em}$) filters. Images captured with the CFP, YFP and FRET filters (F_{CFP}, F_{YFP} and F_{raw}, respectively) were collected every 20 seconds at room temperature using a 40X oil objective (N.A.1.35; Leica) and processed using Slidebook 5.0 software (Intelligent Imaging Innovations). Three-channel corrected FRET was calculated using the following formula: $FRET_c = F_{raw}-F_d/D_d*F_{CFP}-F_a/D_a*F_{YFP}$ where $FRET_c$ represents the corrected energy transfer, F_d/D_d represents measured bleed-through of CFP through the YFP filter (0.44), and F_a/D_a is measured bleed-through of YFP through the CFP filter (0.067). Although the CFP signal was constant in Orai1-CFP stable cells, there was some variation in transiently expressed YFP levels. To compensate for these variations in YFP expression, the above $FRET_c$ values were normalized against acceptor fluorescence (F_{YFP}) to generate N-FRET signals. Thus, N-FRET = $FRET_c/F_{YFP}$. In most figures, the relative changes in N-FRET were compared to resting N-FRET (N-$FRET_{rest}$) levels. This is denoted as ΔN-FRET/N-$FRET_{rest}$, in which ΔN-FRET = N-FRET - N-$FRET_{rest}$. Average FRET measurements shown are typical of at least three independent analyses ± SEM.

2.6. Statistical analyses

Analysis of statistical significance was performed using unpaired Student's t test with GraphPad Prism 5 software. Results are expressed as means ± SEM, *** $p<0.001$.

3. Results

3.1. DPB compounds have high potency and specificity for STIM/Orai-mediated SOCE

Although a great number of studies have described the effects of 2-APB on SOCE mediated by the combined actions of STIM and Orai proteins [1, 57], only one report has appeared on the more potent dimeric 2-APB analogues, DPB162 and DPB163 (Fig. 1) [33]. Our initial studies assessed the effects of these two dimeric borinate compounds on cytosolic Ca^{2+} levels in HEK293 stably transfected with STIM1 and Orai1 (HEK-STIM1-Orai1 cells) loaded with fura-2 (Fig. 2). Using cells in nominally Ca^{2+} free medium, the transient addition of 1 mM external Ca^{2+} resulted in no change in cytosolic Ca^{2+} (Fig. 2A) Addition of the SERCA pump blocker, thapsigargin, caused a release of internal stores and a transient rise in Ca^{2+}. Subsequent readdition of external Ca^{2+} resulted in robust SOCE. Addition of 2 μM DPB162 or DPB163 to cells 2 min prior to adding thapsigargin resulted in almost complete loss of SOCE. We examined the dose-dependence of the action of both compounds using HEK-STIM1-Orai1 cells in similar Ca^{2+} add-back experiments (Fig. S2). The summary of these results (Fig. 2B) reveals that DPB162 inhibits SOCE with an IC_{50} of approximately 200 nM and complete inhibition at 3μM. The dynamics of inhibition with DPB163 were slightly different, with a small enhancement of SOCE at or below 100 nM and inhibition at higher levels with an IC_{50} of approximately 600 nM. We examined the action of 2 μM DPB162 and DPB163 on endogenous SOCE in the RBL-2H3 mast cell line, or the CEM.3-71 or Jurkat T cell lines (Fig. 2C-E). In each case, thapsigargin-mediated SOCE was almost completely inhibited by either compound at 2 μM added at time zero. These actions of DPB162 and DPB163 are in agreement with the results published previously [33] on these compounds for inhibition of both SOCE and the CRAC current mediated by STIM1-induced Orai1 channel activation. Thus, the DPB compounds have approximately 100-fold greater potency than 2-APB which has an IC_{50} of greater than 20 μM [30]. We also assessed reversibility of the actions of DPB162 or 2-APB by applying washout (Fig. S3). The DPB162 effect was still almost complete after 10 min washout whereas the action of 2-APB was largely eliminated. The prolonged action of DPB162 compared with 2-APB may reflect a slower off-rate and would be consistent with its higher potency in blocking STIM/Orai-mediated SOCE.

Importantly, we determined that the DPB compounds, in contrast to 2-APB, have high specificity for store-operated channels among Ca^{2+} permeable channels. We used HEK293 cells expressing the α_{1C}-subunit of the L-type Ca^{2+} channel which gives robust nimodipine-sensitive Sr^{2+} entry in response to depolarization induced by high K^+ [53]. At their maximal SOCE inhibitory level (2 μM), neither of the DPB compounds induced any decrease in L-type channel activity. In contrast, using 2-APB at the lowest

concentration that maximally blocks SOCE (50 μM), there was almost complete block of L-type channel-mediated Ca^{2+} entry (Fig. 3A). We also examined the actions of the DPB compounds on TRPC channel function. These channels have been reported to be store-sensitive, however, the role of the store-sensing STIM proteins in their activation remains controversial [1]. The TRPC3 and TRPC6 channels are characteristically activated by diacylglycerol through a mechanism that is independent of protein kinase C [58]. As shown in Fig. 3B and 3C, the DPB compounds at their maximal SOCE-inhibitory level (2 μM) were without effect on either TRPC3 or TRPC6 channels stably expressed in HEK293 cells and activated by the cell-permeant diacylglycerol analogue, OAG. In contrast, we showed earlier that 2-APB completely blocks the function of TRPC3 and TRPC6 channels when applied at the level that blocks SOCE [32, 34, 59]. This represents an important distinction in specificity between the actions of DPBs and 2-APB. We examined the actions of DPB compounds on Ca^{2+} pumping activity in cells. Earlier reports had suggested that 2-APB could have inhibitory actions on Ca^{2+} pumping in cells [40, 41]. Our results reveal that DPBs did not alter the capacity of Ca^{2+} stores whether added shortly before thapsigargin (Fig. 2A) or pre-incubated for 10 minutes (see subsequent figures). Thus, DPBs did not appear to alter SERCA-mediated Ca^{2+} pumping into stores. We also examined whether the rate of Ca^{2+} pumping out of cells through the action of the PMCA pump was altered by DPBs. As shown in Fig. 3D, in HEK-wildtype cells with stores emptied through prior addition of thapsigargin, Ca^{2+} readdition resulted in robust SOCE. Subsequent addition of EGTA (to buffer external Ca^{2+} to a low level and prevent further Ca^{2+} entry), either with or without DPBs, resulted in the same rates of PMCA-mediated recovery of cytosolic Ca^{2+} levels. Thus, DPBs affect neither PMCA nor SERCA activities.

3.2. Assessment of DPB specificity for STIM and Orai subtypes using STIM or Orai knockout cells.

In the single earlier report on DPB compounds [33], it was noted that they showed considerable specificity among Orai and STIM subtypes. We undertook studies to more definitively investigate such specificity by taking advantage of knockout DT40 chicken B cell lines exclusively expressing specific Orai and STIM protein subtypes. The chicken genome is missing the Orai3 gene and chicken cells express only the Orai1 and Orai2 subtypes. Using the Orai2-knockout DT40 cell line, SOCE mediated exclusively by the Orai1 channel was completely blocked by either DPB162 or DPB163 at 2 μM (Fig. 4A). Using Orai1-knockout DT40 cells, SOCE mediated by Orai2 was considerably less sensitive to addition of DPB compounds. Even 13 min with DPB162 at 300 nM had no effect on Orai-2 mediated SOCE, and 3 μM DPB162 had barely a half-maximal effect (Fig. 4B). Similar insensitivity was seen with DPB163. Limited solubility of the DPB compounds prevented addition at higher levels. Thus, Orai2 appears to have some 10-fold lower sensitivity to the DPB compounds. We initially investigated the actions of DPBs on Orai3 using stable Orai3-expressing HEK293 cells (HEK-Orai3) transfected with

STIM1-YFP (Fig. 4C). We noted considerable SOCE resistance to the DPBs but endogenous Orai1 may have contributed to the DPB-sensitive SOCE component. In contrast to Orai1 and Orai2, the Orai3 channel is well known to be activated by 2-APB without any requirement for STIM proteins [42-46]. Using HEK-Orai3 cells in which stores had not been depleted of Ca^{2+}, while DPB162 had no effect, the addition of 2-APB resulted in a robust activation of Orai3-mediated SOCE which was unaltered by either DPB162 or DPB163 (Fig. 4D). To investigate Orai-3 more directly, we expressed Orai3 in the DT40 Orai1/Orai2 double knockout cell line [46](Fig. 4E). Orai3-expressing DKO cells had robust SOCE compared to a complete lack of SOCE in untransfected cells (Fig. 4E, right) or in Orai3-expressing DKO cells without store-emptying (Fig. 4E, left). The Orai3-mediated SOCE was unaffected by DPB162 or DPB163, providing compelling evidence that Orai3, even in a store-dependent mode, is distinct from Orai1. Intriguingly, despite their potent inhibitory action on SOCE, the powerful direct effect of 2-APB observed by several groups to induce STIM-independent activation of Orai3 channels, was not seen for the DPB compounds.

We extended our specificity studies to compare the actions of DPBs on the function of the two STIM proteins, STIM1 and STIM2. This was important since several significant distinctions in the function and Orai-coupling of STIM1 and STIM2 have been reported [47, 60]. We turned again to the DT40 cell lines in which STIM1 and/or STIM2 genes have been knocked out. Using the STIM2 knockout DT40 line, we observed almost full inhibition of SOCE (Fig. 5A) consistent with a STIM1-mediated Ca^{2+} entry profile. In contrast, the smaller SOCE observed in the STIM1 knockout line was not inhibited by either DPB162 or DPB163 (Fig. 5B). Intriguingly, both compounds showed some activation of STIM2-mediated Ca^{2+} entry. A slight increase at 300 nM was seen with DPB162, and a substantial increase between 100 and 300 nM was seen with DPB163 (Fig. 5C). In the earlier report [33], it was suggested that some of the increased CRAC current observed, especially with DPB163, might have been due to STIM2, but this was from observations on heterologously expressed systems. The results here with knockout cell lines provide definitive information on the stark difference in effects of the DPB compounds on STIM1 and STIM2. We recently revealed important differences between the functional coupling of STIM1 and STIM2 with Orai1 channels [47]. Thus, we hypothesize that the action of DPB compounds is directed toward the site of interaction between STIM and Orai proteins.

3.3. DPB162 blockade of Orai1 activation has no requirement for the STIM1 N-terminal domain

The site of action of DPB compounds was an important question to address. In their earlier study, Goto et al [33] suggested that the DPBs might exert their effects by modifying the store depletion-mediated clustering of STIM1 proteins. The initial sensing of Ca^{2+} depletion and triggering of STIM1 clustering is mediated by the ER luminal N-terminus of STIM1 which contains the Ca^{2+}-sensing EF-hand

regions [1]. Given our hypothesis that DPBs act on the Orai1-coupling site of STIM1, we directed studies toward assessing the actions of DPB162 on the expressed cytoplasmic C-terminal region of STIM1 (STIMct; amino acids 235-685 of STIM1) which contains the Orai1 interacting region. Even though STIM1ct contains the STIM-Orai Activating Region (SOAR; aa 344-442) that binds to and gates Orai channels, when expressed as a soluble cytosolic protein, STIM1ct is a poor activator of Orai1 channels [46, 47]. STIM1ct is missing the luminal ER N-terminus of STIM1 which senses ER Ca^{2+} depletion and undergoes a conformational change that initially triggers STIM1 aggregation and translocation into the ER-PM junctions, and induces a crucial unfolding of the STIM1 C-terminus to expose SOAR and allow it to tether and activate Orai channels [1]. The expressed C-terminal STIM1 domain, lacking the N-terminal triggering process, appears to remain in an inactive, folded state unable to interact with Orai channels [46, 47]. We utilized the constitutively active ST1M1ct-4EA mutant in which four of the acidic residues (E318, E319, E320, E322) in the first coiled-coil distal to the SOAR region, are all mutated to alanines [26]. This appears to prevent the internal folding of the expressed STIM1ct that normally precludes its interaction with Orai1 – likely this unfolding mimics that induced in the holo-STIM1 molecule by store-depletion [21]. Using HEK-Orai1 cells under store replete conditions, STIM1ct-YFP gave rise to almost no Ca^{2+} entry after Ca^{2+} addition (Fig. 6A). In contrast, STIM1ct-4EA-YFP expression resulted in high constitutive Ca^{2+} entry. The preaddition of 2 μM DPB162 inhibited this constitutive Ca^{2+} entry (Fig. 6B). Acute addition of DPB162 after maximal Ca^{2+} entry, caused a rapid decrease of Ca^{2+} (Fig. 6C). These results are important, providing strong evidence that the action of DPB162 on STIM1-induced Orai1 activation does not require the presence of the STIM1 N-terminal domain, nor the emptying of Ca^{2+} stores.

3.4. Functional not physical coupling of dimeric SOAR with Orai1 is blocked by DPB162 and 2-APB

To further pinpoint the actions of DPB162, we examined its effects on the operation of SOAR, the minimal fragment of STIM1 able to functionally couple to Orai1 [10, 11]. In these studies we also compared the actions of DPB162 and 2-APB. SOAR-YFP expressed in HEK-Orai1 cells gave constitutive Ca^{2+} entry rapidly blocked by 50 μM 2-APB (Fig. 7A). Treatment of cells with 2 μM DPB162 was also inhibitory, almost completely blocking SOAR-induced constitutive Ca^{2+} entry (Fig. 7B). Intrinsic FRET between YFP-SOAR and Orai-CFP is high as we recently described [47] since SOAR is avidly bound to Orai1 at the plasma membrane. DPB162 did not induce any change in FRET level and 2-APB increased it slightly (Fig. 7C). As seen in Fig. 7D, expressed YFP-SOAR appears almost exclusively in the plasma membrane and is mostly absent from the cytosol (Fig. 8D, top row). The overlap of YFP-SOAR with Orai1-CFP at the plasma membrane was almost complete as revealed in the merged image. Neither DPB162 addition (Fig. 7D, middle row) nor subsequent 2-APB addition (Fig.

7D, bottom row) caused any obvious change in the tightly overlapping distribution of SOAR and Orai1. Importantly, these FRET and imaging results reveal that DPB and 2-APB do not inhibit SOCE by dissociating the SOAR-Orai1 interaction. We also examined the action of 2 μM DPB162 on the strong FRET signal between holo-STIM1-YFP and Orai-CFP following store-depletion, and observed no change (Fig. S4). Thus, DPB162 at the concentration that maximally blocks SOCE does not alter the store depletion-mediated interaction between full-length STIM1 and Orai1 in ER-PM junctions.

Previous studies show that STIM1 likely exists in a dimeric state, both at rest and in its activation of Orai1 channels [12, 21]. One possibility was the 2-APB or DPB162 might function to inhibit SOAR by preventing or altering the formation of SOAR dimers. Hence we examined the function of a concatemeric construct expressing a YFP-tagged tandem repeat of two SOAR fragments with an intervening 21-amino acid spacer sequence (YFP-SOAR-SOAR), similar to a construct published earlier [61]. Compared with SOAR, we observed that the YFP-SOAR-SOAR protein was more uniformly expressed in HEK-Orai1 cells, giving robust and consistent Ca^{2+} responses (Fig. 7E-G). The dimeric construct mediated SOCE that was rapidly and completely blocked by either 2-APB or DPB162. FRET changes induced by DPB162 were minimal and 2-APB induced a slight FRET increase (Fig. 7H). Neither DPB162 nor 2-APB altered the strong co-association of YFP-SOAR-SOAR with Orai1 at the plasma membrane (Fig. 7I). Again, the data reveal that the block of Ca^{2+} entry by 2-APB or DPB162 is not due to any SOAR-Orai1 dissociation. Since the concatemeric YFP-SOAR-SOAR protein would favor dimer formation, these data provide good evidence that the actions of either DPB162 or 2-APB are unlikely to be mediated by dimer dissociation. However, we further extended the study to examine the effect of DPB162 directly on dimeric association between SOAR subunits. Thus, measuring FRET between co-expressed YFP-SOAR and CFP-SOAR, we observed no alteration by DPB162 (Fig. S5).

3.5. Unlike 2-APB, DPB162 does not promote physical and functional coupling of inactive STIM1ct

A considerable number of studies have documented the unusual biphasic kinetics of the action of 2-APB on STIM/Orai mediated Ca^{2+} signaling [1, 29, 30, 62]. At low μM levels, 2-APB can enhance SOCE, whereas at 50 μM it is strongly inhibitory. The DPB162 molecule, although a simple dimer of 2-APB, shows much higher potency and simpler kinetics on STIM1/Orai1-mediated SOCE (Fig. 2B). A related and remarkable characteristic of the action of 2-APB is its ability to trigger activation of the otherwise inactive STIM1ct molecule. Thus, 2-APB at the concentration (50 μM) which normally completely inhibits SOCE, induces instead a profound activation of the physical interaction between STIM1ct and Orai1 [46, 47]. This 2-APB induced interaction triggers both Ca^{2+} entry and authentic CRAC current mediated by the Orai1 channel, these actions all entirely *independent* of any store-depletion [46, 47]. As shown above (Fig. 6A), HEK-Orai1 cells transiently expressing STIM1ct-YFP,

have no constitutive Ca^{2+} entry. As shown in Fig. 8A, the addition of DPB162 at its maximal SOCE-inhibitory level (2 μM) had no effect. In contrast, the maximal SOCE-inhibitory level of 2-APB (50 μM) induced an acute and profound activation of Ca^{2+} entry. Even with 10-min preincubation, DPB162 did not change Ca^{2+} entry (Fig. 8B). Unexpectedly, added either acutely or with preincubation, DPB162 did *not* block the activating effect of 2-APB on Orai1 function. Examination of FRET between STIM1ct-YFP and Orai1-CFP revealed no DPB162-induced interaction between these proteins in contrast to the rapid, substantial increase in FRET induced by 2-APB (Fig. 8C).

3.6. DPB162 induces dichotomous physical and functional coupling of the Orai1-coupling-defective STIM1-F394H mutant

We extended investigation of this remarkable difference of effect of 2-APB and DPB162 using a mutated form of whole STIM1. We recently identified a residue in the STIM-Orai-activating region (SOAR) of the C-terminal STIM1 domain (Phe-394) that is crucial to both the binding to and activation of Orai1 channels [47]. The single F394H mutation prevents store-induced STIM1-Orai1 FRET and any store-induced activation of Orai1 channels [47]. Importantly, using HEK-Orai1 cells expressing the F394H mutation of STIM1-YFP, addition of 50 μM 2-APB completely overcomes the mutational defect, restoring high STIM-Orai FRET and rapid activation of Orai1 channel function (Fig. 8D-F). This restoring action of 2-APB was reminiscent of its effect described above on STIM1ct, except with STIM1-F394, the effect of 2-APB has an *absolute requirement* for store-depletion [47]. Unlike 2-APB, acute addition of DPB162 had no activating effect on STIM1-F394H (Fig. 8D). Also, DPB162 did not block the effect of 2-APB (Fig. 8D). After a 10 min pre-incubation, a very slight activating effect on SOCE was detected with DPB162 but again no decrease in the 2-APB-induced SOCE activation (Fig. 8E). Examining FRET between Orai1-CFP and STIM1-F394H-YFP, we observed a rapid increase in signal upon addition of DPB162 (Fig. 8F). The FRET signal was further enhanced upon addition of 2-APB. Adding 2-APB alone caused an increase in FRET that was similar to the final FRET signal after the sequential addition of DPB and 2-APB. Thus, DPB162 can promote rapid binding of the STIM1-F394H mutant to Orai1 yet, under the same condition of acute addition, does not trigger Orai1 channel gating.

We continued this investigation by examining the actions of 2-APB and DPB162 on operation of the small SOAR sequence within STIM1 containing the F394H mutation. Expressing YFP-SOAR-F394H in HEK-Orai1 cells, we observed no constitutive Ca^{2+} entry. Addition of 2-APB induced a rapid and transient increase in SOCE similar to the full length mutated STIM1 protein (Fig. 9A), indicating that the restoring action of 2-APB requires only the SOAR fragment of the STIM1 molecule. Acute addition of DPB162 induced a slow but sustained increase in Ca^{2+} entry (Fig. 9B), quite distinct from the rapid, transient Ca^{2+} entry induced by 2-APB. DPB162 induced a rapid and large increase in FRET between

YFP-SOAR-F394H and Orai1-CFP (Fig. 9C) although not as dramatic as 2-APB. Note, the resting FRET values for the wildtype YFP-SOAR were substantially higher than with the mutant YFP-SOAR-F394H, as shown in Fig. 9D. Thus, the single point mutation in the SOAR-F394H mutant is sufficient to give a weak interaction with Orai1 that is rapidly and substantially increased with DPB162 or 2-APB.

We also utilized the dimeric YFP-SOAR-SOAR construct with the F394H mutation in each SOAR unit (YFP-SOAR-FH-SOAR-FH). As mentioned above, this mutated SOAR construct was more stably expressed than SOAR-FH (see Fig. S1). With this construct, 2-APB again induced rapid and transient Ca^{2+} entry (Fig. 9E). Now the effect of DPB162 was faster and larger (Fig. 9F) than with the monomeric SOAR mutant, and was also sustained with time. DPB162 induced a rapid onset of FRET between YFP-SOAR-FH-SOAR-FH and Orai1-CFP (Fig. 9G) although, as for the SOAR monomer, not quite as substantial as that induced by 2-APB. Note, the resting FRET value for the wildtype YFP-SOAR-FH-SOAR-FH / Oria1 interaction was almost 50% higher than the YFP-SOAR-F394H / Orai1 FRET value (Fig. 9D) suggesting it has somewhat enhanced association. Imaging revealed that the YFP-SOAR-FH-SOAR-FH was mostly cytosolic at rest (Fig. 9H top row), and that DPB162 induced substantial movement to the plasma membrane and almost complete overlap with Orai1-CFP (Fig. 9H, center row). Subsequent addition of 2-APB caused little further change (Fig. 9H, bottom row).

These results reveal a clear and remarkable dichotomy between the actions of DPB162 on binding of the SOAR mutant and coupling to Ca^{2+} entry. Like 2-APB, DPB162 induces rapid onset of interaction between the binding-defective SOAR mutant and Orai1. But unlike 2-APB, it appears that DPB162 is unable to rapidly induce the correct gating conformation of Orai1, although the channel slowly opens with time. This dichotomy is more obvious with the single mutant SOAR construct than the mutant double-SOAR construct. Whereas 2-APB induces an immediate activation of Ca^{2+} entry, it is short-lived and rapidly terminates. In contrast the activation induced by DPB162 is stable with time. Clearly, the effectiveness of DPB162 in restoring function to the coupling-defective F394H mutant depends on the actual STIM1 molecule used. With STIM1-F394H, DPB162 restores physical but not functional coupling and requires store-depletion. With SOAR-F394H, DPB162 directly restores rapid physical but very slow functional coupling. With the SOAR-FH-SOARFH dimeric construct, DPB162 restores physical and functional coupling with almost the same kinetics. Likely the mutant dimer has an enhanced binding-configuration as reflected by it higher resting FRET level compared to the mutant monomer. Thus, it appears the SOAR dimer has the most conducive structure for restoration by DP162.

4. Discussion

Our results provide new information on the actions of the DPB molecules on SOCE mediated by STIM and Orai proteins. Our initial studies extended those of Goto *et al* [33] to characterize the kinetics of action of DPBs. In STIM1-Orai1 overexpressing cells, the sensitivity of SOCE to DPB162 or DPB163 was in good agreement with those results. Inhibition by the DPB162 molecule shows simple kinetics with an IC_{50} of approximately 200 nM, some 100-fold more potent than 2-APB [30]. The actions of DPB163 are more complex, lower levels giving slight activation of SOCE, and higher level inhibiting with an IC_{50} of approximately 600 nM. Our studies provide new information on the specificity of action of these agents. The action of DPB162 is of much greater specificity for Orai1-mediated Ca^{2+} entry than 2-APB. Thus, at its maximal inhibitory effect on Ca^{2+} entry mediated by STIM1/Orai1, we show the drug has little effect on L-type Ca^{2+} channels, TRPC channels, Ca^{2+} pumps, or Ca^{2+} leak from ER. This is an important distinction from the many actions that have been described for 2-APB on a variety of Ca^{2+} channels and pumps [31-41]. The results reveal DPB162 as likely the most sensitive and specific blocker of STIM1/Orai1-mediated Ca^{2+} entry yet described. Other classes of compounds including the widely used econazole, SKF-96365, and the 3,5-bis(trifluoromethyl)pyrazole derivative BTP-2 have considerably less specificity and modify other channel activities with similar potency [63-66]

The specificity of action of DPBs among STIM and Orai subtypes is a further significant finding. This was addressed in the earlier overexpression studies of Goto *et al* [33], however the results here utilized DT40 knockout cell lines in which specific STIM and Orai subtypes had been eliminated. The results reveal that DPB162 and DPB163 target Orai1 and Orai2 channels, although their effect on the latter require higher concentrations. Even at high levels, neither DPB162 nor DPB163 blocked Orai3 channels. Among the two STIM subtypes, the potent action of DPBs was remarkably selective for STIM1. Whereas DPB162 had little effect on STIM2, the DPB163 analogue induced a profound activation of STIM2-mediated SOCE over the narrow 100-300 nM range. This suggests that the DPB compounds would be useful tools to selectively probe the actions of STIM2 in store-operated Ca^{2+} signaling responses. However, in most cell systems both STIM1 and STIM2 are expressed and it would be unclear what effect DPBs would exert on heterologously expressed STIM1 and STIM2 which would include mixed STIM1/STIM2 aggregates [67]

In the earlier study [33], it was suggested that in cells expressing STIM1, the action of 2-APB might be to prevent STIM1aggregation. However, we reveal here that the inhibitory action of DPB162 is observed on the cytosolic STIM1ct and SOAR fragments which do not undergo store-dependent aggregation. Moreover, in cells expressing both STIM1 and Orai1, we did not observe any alteration in the ability of STIM1 or Orai1 to move into puncta in response to store-depletion. Hence, the store-

induced aggregation and translocation of STIM1 proteins into Orai1-assocaited ER-PM junctions was not affected.

While DPBs are clearly far more potent and specific blockers of STIM1/Orai1-mediated SOCE than 2-APB, they markedly differ in their effects from the complex actions of 2-APB. The 2-APB molecule, although much weaker in blocking Ca^{2+} entry, is able to "force" the poorly active STIM1ct fragment to bind and activate the Orai1 channel, albeit transiently. Likewise, the full-length STIM1-F394H molecule, mutated at a crucial residue making it defective in both Orai1 binding and gating, is induced by 2-APB to bind to and gate the Orai1 channel. In both cases, 2-APB activates authentic CRAC current [46, 47] hence 2-APB causes inactive STIM1 to induce the correct conformational change in Orai1 that gates its channel activity. DPB162 neither mimics this action of 2-APB on Orai1, nor, curiously, does it block the 2-APB-induced Orai1 gating. This is important indicating that 2-APB has locked-in a STIM1-Orai1 coupling configuration that now excludes the action of DPB162 which is normally a powerful blocker of Orai1 channel activation. We may also conclude that DBP-162 does not function as a simple Orai1 pore-blocking agent.

The blocking action of DPB162 on the activated holo-STIM1 protein appears to be the same as with the SOAR fragment. Studies reveal that the holo-STIM1 molecule unfolds during the store-induced activation process to expose the SOAR moiety [1, 68]. The isolated STIM1ct molecule has not undergone the activation process and is largely inactive [46]. However, the constitutively active STIM1ct-4EA mutant appears to be in the unfolded mode [12, 26] and, like activated holo-STIM1 or SOAR, allows access of DPB162 which prevents Orai1 activation. The observation that DPB162 blocks the action of STIM1ct-4EA suggests that this mutation behaves more like the store depletion-activated holo-STIM1 protein. But this effect of DPB162 is quite distinct from the 2-APB-forced activation of STIM1ct or STIM1-F394H which excludes any blocking action of DPB162.

The coupling interaction between STIM1 and Orai1 is between the short active SOAR segment of STIM1 and a combination of the N- and C-termini of Orai1 [10, 11, 16, 28]. The C-terminal sequence of Orai1 is considered to provide a strong binding site for SOAR and the N-terminus to mediate gating of the channel itself as a consequence of SOAR binding [11, 28]. Recently, the discrete operation of these two Orai1 sites has been reconsidered and instead, the close proximity of the N- and C-termini may create a single binding pocket involving both SOAR-binding and gating of the channel [20, 22, 47]. The DPB162 molecule is likely acting directly on this *coupling interface* between SOAR and Orai1. DPB162 appears to be a potent and specific STIM1/Orai1 *functional uncoupler*. It does not affect the SOAR-

Orai1 interaction, but it potently blocks the SOAR-mediated activation of the Orai1 channel. Yet, its action is not consistent with it directly blocking the Orai1 channel pore. Importantly, the F394H mutation affects both physical interaction between SOAR and Orai1 as well as functional coupling to activate the Orai1 channel. The DPB162 molecule can clearly overcome the binding defect in SOAR-F394H, allowing rapid association between the two. But it does not immediately overcome the functional coupling defect between the two proteins. With SOAR-F394H, it slowly induces Orai1 channel opening; with SOAR-FH-SOAR-FH, it does this more rapidly since, presumably, the dimer is in a configuration closer to that needed for activation. With STIM1-F394H, the return of functional coupling is even slower than SOAR-F394H, likely reflecting a further constraint imposed by in the environment of the whole STIM1 molecule. The fact that DPB162 can induce a dissociation between physical binding and functional coupling in the F394H mutation indicates the two processes are intimately linked and crucially mediated by this site on SOAR. Indeed, 2-APB induces a profound and simultaneous activation of both physical and functional coupling of the mutant, reflecting its higher efficacy for the defect rendered by F394H. Although we have not yet pinpointed the precise molecular nature of the SOAR-Orai1 functional coupling event, the DPB162 and 2-APB molecules are clearly important structural probes for investigating this site further in structural studies.

An interesting further clue to the site of action of DPB162 is its very different effect on STIM1 as opposed to STIM2. From our recent work, we revealed that STIM1 and STIM2 have a crucial difference at the F394 locus of SOAR. In STIM2, this site is a leucine, and considerably decreases its functional coupling to Orai1 [47]. It is likely that this is the molecular basis for the difference in action of DPB162 on STIM1 and STIM2. Thus, DPB162 may be useful in further probing the differences in Orai1-coupling between STIM1 and STIM2. The lack of effect of DPB162 on Orai3 is another interesting facet of its mode of operation. Orai3 can be directly activated by 2-APB without STIM1 [42-46], its action partially mimicking the function of STIM1 and likely functioning on the Orai3 coupling interface to STIM proteins. The lack of action of DPB162 may again provide important information on the distinct coupling site in Orai3.

Overall, we conclude that the actions of both DPB162 and 2-APB are directed toward the STIM-Orai coupling moieties that mediate the key conformational change that occurs as STIM proteins tether and gate Orai channels. It seems the action of both molecules is highly dependent on the precise configuration of the STIM-Orai interface. Their mixed activation and inhibition profiles most likely reflect a fine line between promoting as opposed to preventing successful coupling to Orai channels.

Acknowledgements

This work was funded by NIH grants AI058173 and GM109279 (DLG), and the National Natural Science foundation of China (NSFC-31471279) and Program for New Century Excellent Talents in University, NCET-13-0061 (YW).

References

[1] J. Soboloff, B.S. Rothberg, M. Madesh, D.L. Gill, STIM proteins: dynamic calcium signal transducers, Nat Rev Mol Cell Biol, 13 (2012) 549-565.

[2] B.A. McNally, M. Prakriya, Permeation, selectivity and gating in store-operated CRAC channels, J Physiol, 590 (2012) 4179-4191.

[3] P. Kar, C. Nelson, A.B. Parekh, CRAC Channels Drive Digital Activation and Provide Analog Control and Synergy to Ca^{2+}-Dependent Gene Regulation, Curr Biol, 22 (2012) 242-247.

[4] R.S. Lewis, Store-operated calcium channels: new perspectives on mechanism and function, Cold Spring Harbor perspectives in biology, 3 (2011) 1-24.

[5] S. Feske, E.Y. Skolnik, M. Prakriya, Ion channels and transporters in lymphocyte function and immunity, Nat Rev Immunol, 12 (2012) 532-547.

[6] P.J. Shaw, S. Feske, Regulation of lymphocyte function by ORAI and STIM proteins in infection and autoimmunity, J Physiol, 590 (2012) 4157-4167.

[7] P.G. Hogan, R.S. Lewis, A. Rao, Molecular basis of calcium signaling in lymphocytes: STIM and ORAI, Annu Rev Immunol, 28 (2010) 491-533.

[8] P.B. Stathopulos, L. Zheng, G.Y. Li, M.J. Plevin, M. Ikura, Structural and mechanistic insights into STIM1-mediated initiation of store-operated calcium entry, Cell, 135 (2008) 110-122.

[9] L. Zheng, P.B. Stathopulos, R. Schindl, G.Y. Li, C. Romanin, M. Ikura, Auto-inhibitory role of the EF-SAM domain of STIM proteins in store-operated calcium entry, Proc Natl Acad Sci U S A, 108 (2011) 1337-1342.

[10] J.P. Yuan, W. Zeng, M.R. Dorwart, Y.J. Choi, P.F. Worley, S. Muallem, SOAR and the polybasic STIM1 domains gate and regulate Orai channels, Nat Cell Biol, 11 (2009) 337-343.

[11] C.Y. Park, P.J. Hoover, F.M. Mullins, P. Bachhawat, E.D. Covington, S. Raunser, T. Walz, K.C. Garcia, R.E. Dolmetsch, R.S. Lewis, STIM1 clusters and activates CRAC channels via direct binding of a cytosolic domain to Orai1, Cell, 136 (2009) 876-890.

[12] X. Yang, H. Jin, X. Cai, S. Li, Y. Shen, Structural and mechanistic insights into the activation of Stromal interaction molecule 1 (STIM1), Proc Natl Acad Sci U S A, 109 (2012) 5657-5662.

[13] A. Penna, A. Demuro, A.V. Yeromin, S.L. Zhang, O. Safrina, I. Parker, M.D. Cahalan, The CRAC channel consists of a tetramer formed by Stim-induced dimerization of Orai dimers, Nature, 456 (2008) 116-120.
[14] M. Muik, M. Fahrner, I. Derler, R. Schindl, J. Bergsmann, I. Frischauf, K. Groschner, C. Romanin, A cytosolic homomerization and a modulatory domain within STIM1 C-terminus determine coupling to ORAI1 channels, J. Biol. Chem., 284 (2009) 8421-8426.
[15] E.D. Covington, M.M. Wu, R.S. Lewis, Essential role for the CRAC activation domain in store-dependent oligomerization of STIM1, Mol Biol Cell, 21 (2010) 1897-1907.
[16] X. Hou, L. Pedi, M.M. Diver, S.B. Long, Crystal structure of the calcium release-activated calcium channel Orai, Science, 338 (2012) 1308-1313.
[17] B.A. McNally, M. Yamashita, A. Engh, M. Prakriya, Structural determinants of ion permeation in CRAC channels, Proc Natl Acad Sci U S A, 106 (2009) 22516-22521.
[18] Y. Zhou, S. Ramachandran, M. Oh-Hora, A. Rao, P.G. Hogan, Pore architecture of the ORAI1 store-operated calcium channel, Proc Natl Acad Sci U S A, 107 (2010) 4896-4901.
[19] S.L. Zhang, A.V. Yeromin, J. Hu, A. Amcheslavsky, H. Zheng, M.D. Cahalan, Mutations in Orai1 transmembrane segment 1 cause STIM1-independent activation of Orai1 channels at glycine 98 and channel closure at arginine 91, Proc Natl Acad Sci U S A, 108 (2011) 17838-17843.
[20] B.A. McNally, A. Somasundaram, M. Yamashita, M. Prakriya, Gated regulation of CRAC channel ion selectivity by STIM1, Nature, 482 (2012) 241-245.
[21] B.S. Rothberg, Y. Wang, D.L. Gill, Orai channel pore properties and gating by STIM: implications from the Orai crystal structure, Sci Signal, 6 (2013) pe9.
[22] B.A. McNally, A. Somasundaram, A. Jairaman, M. Yamashita, M. Prakriya, The C- and N-terminal STIM1 binding sites on Orai1 are required for both trapping and gating CRAC channels, J Physiol, (2013).
[23] Z. Li, J. Lu, P. Xu, X. Xie, L. Chen, T. Xu, Mapping the interacting domains of STIM1 and Orai1 in CRAC channel activation, J. Biol. Chem., 282 (2007) 29448-20456.
[24] M. Muik, I. Frischauf, I. Derler, M. Fahrner, J. Bergsmann, P. Eder, R. Schindl, C. Hesch, B. Polzinger, R. Fritsch, H. Kahr, J. Madl, H. Gruber, K. Groschner, C. Romanin, Dynamic coupling of the putative coiled-coil domain of ORAI1 with STIM1 mediates ORAI1 channel activation, J. Biol. Chem., 283 (2008) 8014-8022.
[25] N. Calloway, D. Holowka, B. Baird, A basic sequence in STIM1 promotes Ca^{2+} influx by interacting with the C-terminal acidic coiled coil of Orai1, Biochemistry, 49 (2010) 1067-1071.
[26] M.K. Korzeniowski, I.M. Manjarres, P. Varnai, T. Balla, Activation of STIM1-Orai1 involves an intramolecular switching mechanism, Sci Signal, 3 (2010) ra82.

[27] A. Lis, S. Zierler, C. Peinelt, A. Fleig, R. Penner, A single lysine in the N-terminal region of store-operated channels is critical for STIM1-mediated gating, J Gen Physiol, 136 (2010) 673-686.
[28] H. Zheng, M.H. Zhou, C. Hu, E. Kuo, X. Peng, J. Hu, L. Kuo, S.L. Zhang, Differential Roles of the C and N Termini of Orai1 Protein in Interacting with Stromal Interaction Molecule 1 (STIM1) for Ca^{2+} Release-activated Ca^{2+} (CRAC) Channel Activation, J Biol Chem, 288 (2013) 11263-11272.
[29] M. Prakriya, R.S. Lewis, Potentiation and inhibition of Ca^{2+} release-activated Ca^{2+} channels by 2-aminoethyldiphenyl borate (2-APB) occurs independently of IP_3 receptors, J. Physiol., 536 (2001) 3-19.
[30] H.T. Ma, K. Venkatachalam, J.B. Parys, D.L. Gill, Modification of store-operated channel coupling and inositol trisphosphate receptor function by 2-aminoethoxydiphenyl borate in DT40 lymphocytes, J. Biol. Chem., 277 (2002) 6915-6922.
[31] T. Maruyama, T. Kanaji, S. Nakade, T. Kanno, K. Mikoshiba, 2APB, 2-aminoethoxydiphenyl borate, a membrane-penetrable modulator of Ins(1,4,5)P3-induced Ca2+release, J.Biochem.(Tokyo.), 122 (1997) 498-505.
[32] H.T. Ma, R.L. Patterson, D.B. van Rossum, L. Birnbaumer, K. Mikoshiba, D.L. Gill, Requirement of the inositol trisphosphate receptor for activation of store-operated Ca2+ channels, Science, 287 (2000) 1647-1651.
[33] J. Goto, A.Z. Suzuki, S. Ozaki, N. Matsumoto, T. Nakamura, E. Ebisui, A. Fleig, R. Penner, K. Mikoshiba, Two novel 2-aminoethyl diphenylborinate (2-APB) analogues differentially activate and inhibit store-operated Ca^{2+} entry via STIM proteins, Cell Calcium, 47 (2010) 1-10.
[34] D.B. van Rossum, R.L. Patterson, H.T. Ma, D.L. Gill, Ca2+ entry mediated by store-depletion, S -nitrosylation, and TRP3 channels: Comparison of coupling and function J. Biol. Chem., 275 (2000) 28562-28568.
[35] S.Z. Xu, F. Zeng, G. Boulay, C. Grimm, C. Harteneck, D.J. Beech, Block of TRPC5 channels by 2-aminoethoxydiphenyl borate: a differential, extracellular and voltage-dependent effect, Br J Pharmacol, 145 (2005) 405-414.
[36] K. Togashi, H. Inada, M. Tominaga, Inhibition of the transient receptor potential cation channel TRPM2 by 2-aminoethoxydiphenyl borate (2-APB), Br J Pharmacol, 153 (2008) 1324-1330.
[37] M. Naziroglu, C. Ozgul, O. Celik, B. Cig, E. Sozbir, Aminoethoxydiphenyl borate and flufenamic acid inhibit Ca2+ influx through TRPM2 channels in rat dorsal root ganglion neurons activated by ADP-ribose and rotenone, The Journal of membrane biology, 241 (2011) 69-75.
[38] G. Kovacs, N. Montalbetti, A. Simonin, T. Danko, B. Balazs, A. Zsembery, M.A. Hediger, Inhibition of the human epithelial calcium channel TRPV6 by 2-aminoethoxydiphenyl borate (2-APB), Cell Calcium, 52 (2012) 468-480.

[39] R. Chokshi, P. Fruasaha, J.A. Kozak, 2-aminoethyl diphenyl borinate (2-APB) inhibits TRPM7 channels through an intracellular acidification mechanism, Channels (Austin), 6 (2012) 362-369.
[40] C.M. Peppiatt, T.J. Collins, L. Mackenzie, S.J. Conway, A.B. Holmes, M.D. Bootman, M.J. Berridge, J.T. Seo, H.L. Roderick, 2-Aminoethoxydiphenyl borate (2-APB) antagonises inositol 1,4,5-trisphosphate-induced calcium release, inhibits calcium pumps and has a use-dependent and slowly reversible action on store-operated calcium entry channels, Cell Calcium, 34 (2003) 97-108.
[41] J.G. Bilmen, L.L. Wootton, R.E. Godfrey, O.S. Smart, F. Michelangeli, Inhibition of SERCA Ca2+ pumps by 2-aminoethoxydiphenyl borate (2-APB). 2-APB reduces both Ca2+binding and phosphoryl transfer from ATP, by interfering with the pathway leading to the Ca2+-binding sites, European Journal of Biochemistry, 269 (2002) 3678-3687.
[42] C. Peinelt, A. Lis, A. Beck, A. Fleig, R. Penner, 2-Aminoethoxydiphenyl borate directly facilitates and indirectly inhibits STIM1-dependent gating of CRAC channels, J. Physiol., 586 (2008) 3061-3073.
[43] R. Schindl, J. Bergsmann, I. Frischauf, I. Derler, M. Fahrner, M. Muik, R. Fritsch, K. Groschner, C. Romanin, 2-aminoethoxydiphenyl borate alters selectivity of orai3 channels by increasing their pore size, J. Biol. Chem., 283 (2008) 20261-20267.
[44] S.L. Zhang, J.A. Kozak, W. Jiang, A.V. Yeromin, J. Chen, Y. Yu, A. Penna, W. Shen, V. Chi, M.D. Cahalan, Store-dependent and -independent modes regulating Ca^{2+} release-activated Ca^{2+} channel activity of human Orai1 and Orai3, J. Biol. Chem., 283 (2008) 17662-17671.
[45] W.I. Dehaven, J.T. Smyth, R.R. Boyles, G.S. Bird, J.W. Putney, Jr., Complex Actions of 2-Aminoethyldiphenyl Borate on Store-operated Calcium Entry, J. Biol. Chem., 283 (2008) 19265-19273.
[46] Y. Wang, X. Deng, Y. Zhou, E. Hendron, S. Mancarella, M.F. Ritchie, X.D. Tang, Y. Baba, T. Kurosaki, Y. Mori, J. Soboloff, D.L. Gill, STIM protein coupling in the activation of Orai channels, Proc Natl Acad Sci U S A, 106 (2009) 7391-7396.
[47] X. Wang, Y. Wang, Y. Zhou, E. Hendron, S. Mancarella, M.D. Andrake, B.S. Rothberg, J. Soboloff, D.L. Gill, Distinct Orai-coupling domains in STIM1 and STIM2 define the Orai-activating site, Nature communications, 5 (2014) 3183.
[48] H. Zhou, H. Iwasaki, T. Nakamura, K. Nakamura, T. Maruyama, S. Hamano, S. Ozaki, A. Mizutani, K. Mikoshiba, 2-Aminoethyl diphenylborinate analogues: selective inhibition for store-operated Ca2+ entry, Biochem Biophys Res Commun, 352 (2007) 277-282.
[49] J. Soboloff, M.A. Spassova, T. Hewavitharana, L.P. He, W. Xu, L.S. Johnstone, M.A. Dziadek, D.L. Gill, STIM2 is an inhibitor of STIM1-mediated store-operated Ca^{2+} Entry, Curr. Biol., 16 (2006) 1465-1470.
[50] T. Hewavitharana, X. Deng, Y. Wang, M.F. Ritchie, G.V. Girish, J. Soboloff, D.L. Gill, Location and function of STIM1 in the activation of Ca^{2+} entry signals, J. Biol. Chem., 283 (2008) 26252-26262.

[51] M.A. Spassova, T. Hewavitharana, R.A. Fandino, A. Kaya, J. Tanaka, D.L. Gill, Voltage gating at the selectivity filter of the Ca^{2+} release-activated Ca^{2+} channel induced by mutation of the Orai1 protein, J. Biol. Chem., 283 (2008) 14938-14945.
[52] J. Soboloff, M.A. Spassova, X.D. Tang, T. Hewavitharana, W. Xu, D.L. Gill, Orai1 and STIM reconstitute store-operated calcium channel function, J. Biol. Chem., 281 (2006) 20661-20665.
[53] Y. Wang, X. Deng, S. Mancarella, E. Hendron, S. Eguchi, J. Soboloff, X.D. Tang, D.L. Gill, The calcium store-sensor, STIM1, reciprocally controls Orai and $Ca_V1.2$ channels, Science, 330 (2010) 105-109.
[54] S. Mancarella, Y. Wang, X. Deng, G. Landesberg, R. Scalia, R.A. Panettieri, K. Mallilankaraman, X.D. Tang, M. Madesh, D.L. Gill, Hypoxia-induced acidosis uncouples the STIM-Orai calcium signaling complex, J Biol Chem, 286 (2011) 44788-44798.
[55] Y. Baba, K. Hayashi, Y. Fujii, A. Mizushima, H. Watarai, M. Wakamori, T. Numaga, Y. Mori, M. Iino, M. Hikida, T. Kurosaki, Coupling of STIM1 to store-operated Ca^{2+} entry through its constitutive and inducible movement in the endoplasmic reticulum, Proc. Natl. Acad. Sci. USA, 103 (2006) 16704-16709.
[56] S. Mancarella, S. Potireddy, Y. Wang, H. Gao, R.K. Gandhirajan, M. Autieri, R. Scalia, Z. Cheng, H. Wang, M. Madesh, S.R. Houser, D.L. Gill, Targeted STIM deletion impairs calcium homeostasis, NFAT activation, and growth of smooth muscle, FASEB J, [Epub Nov 20, 2012] (2012).
[57] I. Bogeski, D. Al-Ansary, B. Qu, B.A. Niemeyer, M. Hoth, C. Peinelt, Pharmacology of ORAI channels as a tool to understand their physiological functions, Expert review of clinical pharmacology, 3 (2010) 291-303.
[58] K. Venkatachalam, F. Zheng, D.L. Gill, Regulation of canonical transient receptor potential (TRPC) channel function by diacylglycerol and protein kinase C, J. Biol. Chem., 278 (2003) 29031-29040.
[59] K. Venkatachalam, H.T. Ma, D.L. Ford, D.L. Gill, Expression of functional receptor-coupled TRPC3 channels in DT40 triple InsP 3 receptor-knockout cells, J. Biol. Chem., 276 (2001) 33980-33985.
[60] O. Brandman, J. Liou, W.S. Park, T. Meyer, STIM2 is a feedback regulator that stabilizes basal cytosolic and endoplasmic reticulum Ca^{2+} levels, Cell, 131 (2007) 1327-1339.
[61] Z. Li, L. Liu, Y. Deng, W. Ji, W. Du, P. Xu, L. Chen, T. Xu, Graded activation of CRAC channel by binding of different numbers of STIM1 to Orai1 subunits, Cell Res, 21 (2011) 305-315.
[62] X. Deng, Y. Wang, Y. Zhou, J. Soboloff, D.L. Gill, STIM and Orai - dynamic intermembrane coupling to control cellular calcium signals, J. Biol. Chem., 284 (2009) 22501-22505.
[63] L.P. He, T. Hewavitharana, J. Soboloff, M.A. Spassova, D.L. Gill, A functional link between store-operated and TRPC channels revealed by the 3,5-bis(trifluoromethyl)pyrazole derivative, BTP2, J. Biol. Chem., 280 (2005) 10997-11006.

[64] R. Takezawa, H. Cheng, A. Beck, J. Ishikawa, P. Launay, H. Kubota, J.P. Kinet, A. Fleig, T. Yamada, R. Penner, A pyrazole derivative potently inhibits lymphocyte Ca2+ influx and cytokine production by facilitating transient receptor potential melastatin 4 channel activity, Mol Pharmacol, 69 (2006) 1413-1420.
[65] C. Harteneck, M. Gollasch, Pharmacological modulation of diacylglycerol-sensitive TRPC3/6/7 channels, Current pharmaceutical biotechnology, 12 (2011) 35-41.
[66] M. Song, D. Chen, S.P. Yu, The TRPC channel blocker SKF 96365 inhibits glioblastoma cell growth by enhancing reverse mode of the Na(+) /Ca(2+) exchanger and increasing intracellular Ca(2+), Br J Pharmacol, 171 (2014) 3432-3447.
[67] M.A. Dziadek, L.S. Johnstone, Biochemical properties and cellular localisation of STIM proteins, Cell Calcium, (2007).
[68] A. Gudlur, Y. Zhou, P.G. Hogan, STIM-ORAI interactions that control the CRAC channel, Current topics in membranes, 71 (2013) 33-58.

Figure Legends

Fig. 1. Structures of 2-APB and DPBs. DPB162-AE and DPB163-AE are methyl ether-linked dimers of 2-APB.

Fig. 2. DPB-induced inhibition of SOCE in HEK293 cells and hematopoietic cell lines. (A) Fura-2 Ca^{2+} responses in HEK cells stably expressing STIM1 and Orai1 (HEK-STIM1-Orai1 cells). Ca^{2+}-free solution was changed to 1 mM Ca^{2+}, then removed and readded as shown (bars). Cells were treated with 2 μM DPB162 (red) or DPB163 (green), followed by addition of 2 μM thapsigargin (TG) (arrows). (B) Normalized dose response curves for DPB162 (red) or DPB163 (green) on SOCE in HEK-STIM1-Orai1 cells, from measurements as shown in Fig. S2. Cells were pretreted 12 min with DPBs and 10 min 2 μM TG, as in (A); means ± SEM of peak Ca^{2+} entry from 3 repeats. (C-E) Fura-2 Ca^{2+} responses in hematopoietic cell lines RBL-2H3 mast cells (C), CEM3.71 T cells, (D) and Jurkat T cells (E). Cells were treated with 2 μM TG (10min) in Ca^{2+} free solution, prior to each experiment. 2 μM DPB162 (red) or DPB163 (green) or DMSO (black) were added at t=0, followed by 1 mM Ca^{2+} addition (bar). Control: black; 2 μM DPB162: red; 2 μM DPB163: green. Results are means ± SEM of 10-30 cells per field and results are typical of at least 3 independent experiments.

Fig. 3. DPBs do not affect TRPC channel, L-type channel or PMCA pump activities. Fura-2 cytosolic Ca^{2+} measurement were made on HEK cells stably overexpressing $Ca_V1.2\alpha_{1C}$ (A), TRPC3 (B), TRPC6 (C) or co-expressing STIM1 and Orai1 (D). (A) Fura-2 response of $Ca_V1.2$ channel-mediated Sr^{2+} entry in cells pretreated 5 min with DMSO (black), 2 μM DPB162 (red), 2 μM DPB163 (green) or 50 μM 2-APB (purple). Channel activity was induced by depolarization with 134 mM external K^+ with 3 mM Sr^{2+}, and inhibited by 2 μM nimodipine. (B and C) Fura-2 Ca^{2+} responses in stably-expressing TRPC3 (B) or TRPC6 (C) HEK cells pre-incubated 5 min with DMSO (black), 2 μM DPB162 (red), or 2 μM DPB163 (green). After addition of 3 mM Ca^{2+} (arrow) channel activity was induced with 100 μM OAG (arrow). (D) Fura-2 Ca^{2+} responses in HEK-STIM1-Orai1 cells with stores depleted with 2 μM TG 10 min prior to recording. 1 mM Ca^{2+} addition (arrow) was replaced with Ca^{2+} -free medium containing 1 mM EGTA (arrow). 2μM DPB162 (red), 2 μM DPB163 (green) or DMSO (black) were applied with EGTA. Ca^{2+} imaging responses are means ± SEM of 10-30 cells per field and results are typical of at least 3 independent experiments.

Fig. 4. Orai-channel specificity of action of DPBs measured in DT40 knockout B cells. (A) Fura-2 Ca^{2+} responses in DT40-Orai2 KO cells. Ca^{2+} free solution was replaced with 1 mM Ca^{2+} (bar) applied and removed as shown. 2 μM TG and 2 μM DPB162, or 2μM DPB163 were added as shown (arrows). (B) Hamamatsu FDSS μCell plate reader fluo-4 Ca^{2+} measurements of DT40-Orai1 KO cells. In Ca^{2+} free solution, 2 μM TG and indicated DPB additions were applied 13 min before 3 mM Ca^{2+} addition (bars). DPB162 (left) or DPB163 (right) concentrations were as shown. (C) Fura-2 response in Orai3 stably-expressing HEK cells transiently transfected with STIM1. Ca^{2+} free solution was replaced with 1 mM Ca^{2+} (bars); additions of 2 μM DPB162-AE (red) or DPB163-AE (green), DMSO (black) or 2 μM TG were as shown (arrows). (D) Fura-2 Ca^{2+} responses in Ca^{2+} store-replete HEK cells transiently transfected with Orai3. 1 mM Ca^{2+} addition or removal (bar), 2 μM DPBs (red, green) or DMSO (black), and 50μM 2-APB were applied as shown (arrows). (E) Fura-2 Ca^{2+} responses in Ca^{2+} store-replete (left) or store-depleted (right) DT40-Orai1/2 double knockout cells transiently transfected with Orai3. 2 μM DPBs (red, green) or DMSO (black), or 2 μM TG (right only) were applied 10 min prior to the start of experiment. Note: in the right panel, cells on the same coverslip without CFP fluorescence (no Orai3 transfected) have no Ca^{2+} entry. Ca^{2+} imaging responses are means ± SEM of 10-30 cells per field, and typical of at least 3 independent experiments.

Fig. 5. DPBs selectively inhibit STIM1 but not STIM2 in STIM1 or STIM2 DT40 knockout cells. (A) Fura-2 cytosolic Ca^{2+} responses in DT40-STIM2 KO cells. Ca^{2+} free solution was replaced with1 mM Ca^{2+} as shown (bar). 2 μM TG (10 min) and 2 μM DPB162 (2 min, red) or 2 μM DPB163 (2 min, green) were added prior to re-addition of 1mM Ca^{2+}. (B) Hamamatsu FDSS μCell plate reader Ca^{2+} measurements in DT40-STIM1 KO cells. In Ca^{2+} free solution, 2 μM TG or indicated conctractions of DPB162 (left) or DPB163 (right) were applied 13min before 3 mM Ca^{2+} addition. Cytosolic Ca^{2+} was measured with Fluo-4. (C) Dose-response curves for the average ± SEM of peak Ca^{2+} entry of DPB162 (red) or DPB163 (green) from (B). Results are means ± SEM of multiple cells per field. Results are typical of at least 3 independent experiments.

Fig. 6. DPB162-induced inhibition of constitutive Ca^{2+} entry mediated by STIM1ct-4EA-YFP. (A) Comparison of fura-2 Ca^{2+} responses in HEK-Orai1 cells transfected with either STIM1ct-YFP (black) or STIM1ct-4EA-YFP (blue). Ca^{2+}-free medium was replaced with 1 mM Ca^{2+} (bar). (B) Left: Fura-2 responses in HEK-Orai1 cells transfected with STIM1ct-4EA-YFP, with DMSO (blue) or 2 μM DPB162 (red) added for 10 min. Right panel: average ± SEM peak Ca^{2+} from left panel. (C) Left: Fura-2 response after acute addition of 2 μM DPB162 (arrow) in HEK-Orai cells expressing STIM1ct-4EA-YFP. Right: average ± SEM peak constitutive Ca^{2+} entry (blue) and average ± SEM Ca^{2+} entry 5min after 2 μM

DPB163 addition (red). Results are means ± SEM of 10-30 cells per field, are typical of at least 3 independent experiments. ***, $p<0.001$; unpaired Student's t test.

Fig. 7. DPB162 inhibits functional coupling between SOAR and Orai1. HEK-Orai1 cells were transfected with YFP-SOAR (A-D) or YFP-SOAR-SOAR (E-I). Fura-2 Ca^{2+} responses of YFP-SOAR-induced constitutive Ca^{2+} entry with 10 min treatment with DMSO (A) or 2 μM DPB162 (B) measured with Ca^{2+}-free medium replaced with 1 mM Ca^{2+} as shown (bar) followed by 50 μM 2-APB (arrow). (C) Change in FRET ($\Delta FRET/FRET_{rest}$%) between Orai-CFP and YFP-SOAR in response to DMSO (blue) or 2 μM DPB162 (red), and 50 μM 2-APB (arrow). (D) Fluorescence imaging of YFP-SOAR and Orai1-CFP at rest (top row), after 5min incubation with 2 μM DPB162 (middle), or a further 5min with 50 μM 2-APB (lower). Fura-2 responses of YFP-SOAR-SOAR-induced constitutive Ca^{2+} entry with DMSO (E) or 2 μM DPB162 (F) added 10 min prior to 50 μM 2-APB; 1 mM Ca^{2+} addition as show (bar). (G) Fura-2 Ca^{2+} response of constitutive Ca^{2+} entry with acute addition of 2 μM DPB162. Ca^{2+}-free medium, solution was replaced with 1 mM Ca^{2+} (bar). (H) Change in FRET ($\Delta FRET/FRET_{rest}$%) between Orai-CFP and YFP-SOAR-SOAR in response to DMSO (blue) or 2 μM DPB162 (red), and 50 μM 2-APB (arrow). (I) Fluorescence imaging of YFP-SOAR-SOAR and Orai1-CFP at rest (top row), after 5min application of 2 μM DPB162 (middle row) or 5min further with 50 μM 2-APB. Blue: DMSO; Red, 2 μM DPB. Ca^{2+} imaging and FRET responses are means ± SEM of multiple cells per field, typical of at least 3 independent experiments.

Fig. 8. Actions of DPB162 and 2-APB on Ca^{2+} responses and FRET interactions of coupling-inactive STIM1ct-YFP or STIM1-F394H-YFP proteins expressed in HEK-Orai1 cells. HEK-Orai1 cells were transfected with STIM1ct-YFP (A-C) or STIM1-F394H-YFP (D-F). (A) Fura-2 measurements were in Ca^{2+} free medium, with addition of 1 mM extracellular Ca^{2+}, followed by acute addition of 2 μM DPB162 (red) or DMSO (blue), and 50 μM 2-APB (arrows). (B) Cells as in (A) were preincubated with 2 μM DPB162 (red) or DMSO (blue) for 9 min. 1 mM Ca^{2+} and 50 μM 2-APB were added as shown (arrows). Maximum 2-APB-induced Ca^{2+} levels from 3 experiments were quantified (right panel). (C) Change in FRET ($\Delta FRET/FRET_{rest}$%) between Orai-CFP and STIM1ct-YFP in response to DMSO (blue) or 2 μM DPB162 (red), and 50 μM 2-APB (arrow). (D) Fura-2 measurements in Ca^{2+} free medium, with addition of 2 μM TG, 1 mM extracellular Ca^{2+}, followed by acute addition of 2 μM DPB162 (red) or DMSO (blue), and 50 μM 2-APB (arrows). (E) Preaddition of 2 μM DPB162 (red) or DMSO (blue) was 20 sec before recording; fura-2 measurements were in Ca^{2+}-free medium, with addition of 2 μM TG, 1 mM extracellular Ca^{2+} and 50 μM 2-APB (arrows). Maximum 2-APB-induced Ca^{2+} increase from 3 experiments was quantified (right panel). (F) Change in FRET ($\Delta FRET/FRET_{rest}$%) between Orai-CFP and STIM1-F394H-YFP in response to 2 μM TG, DMSO (blue) or 2 μM DPB162 (red), and 50 μM 2-

APB (arrows). Ca^{2+} imaging and FRET responses are means ± SEM of multiple cells per field and results are typical of at least 3 independent experiments. P>0.05; unpaired Student's t test.

Fig. 9. Dichotomous DPB162-induced restoration of Orai1 FRET interactions and Orai channel activation by Orai1 coupling-defective mutant SOAR-F394H proteins. (A-C) Fura-2 Ca^{2+} measurements or FRET measurements in HEK-Orai1 cells transfected with YFP-SOAR-F394H. Ca^{2+} responses after 1 mM Ca^{2+} (bar), and either DMSO (A) or 2 μM DPB162 (B), followed by 50 μM 2-APB (arrows). (C) Change in FRET ($\Delta FRET/FRET_{rest}$%) between Orai-CFP and YFP-SOAR-F394H in response to DMSO (blue) or 2 μM DPB162 (red), and 50 μM 2-APB (arrow). (D) Mean resting N-$FRET_{rest}$ measured in HEK-Orai1 cells between Orai1-CFP and either YFP-SOAR (red), YFP-SOAR-F394H (green), YFP-SOAR-SOAR (turquoise), or YFP-SOAR-FH-SOAR-FH (orange). (E-H) As above except HEK-Orai1 cells were transfected with YFP-SOAR-FH-SOAR-FH. Ca^{2+} responses after 1 mM Ca^{2+} (bar), and either DMSO (A) or 2 μM DPB162 (B), followed by 50 μM 2-APB (arrows). (C) Change in FRET ($\Delta FRET/FRET_{rest}$%) between Orai-CFP and YFP-SOAR-FH-SOAR-FH in response to DMSO (blue) or 2 μM DPB162 (red), and 50 μM 2-APB (arrow). (H) Colocalization of YFP-SOAR-FH-SOAR-FH and Orai1-CFP either at rest (top row), 5 min after DPB162, or a further 5 min with 50 μM 2-APB added. Ca^{2+} imaging and FRET responses are means ± SEM of multiple cells per field, typical of at least 3 independent experiments. ***, p<0.001; unpaired Student's t test.

Supplemental Figure Legends

Fig. S1: Expression of YFP-SOAR and YFP-SOAR-SOAR constructs in HEK-Orai1 cells. (A) Western analysis of expression of YFP-SOAR and YFP-SOAR-F394H. (B) Expression of YFP-SOAR and YFP-SOAR-SOAR constructs in HEK-Orai1 cells by measuring YFP-fluorescence intensity per transfected cell. Numbers above columns refer to transfection efficiency, i.e. the number of cells showing detectable fluorescence vs. the total number of cells. For most constructs, this was approximately 50%. For cells expressing the YFP-SOAR-F394H construct, this was substantially less (approx.. 14%). However, the fluorescence intensity per cell was only 30% less than for YFP-SOAR-expressing cells.

Fig. S1. Dose-response curves of DPB162 (A) or DPB163 (B) effects on SOCE in HEK-STIM1-Orai1 cells. Typical Fura-2 ratiometric responses of cytosolic Ca^{2+} as averaged in Fig. 1B. Cells were pre-incubated with DPBs (12min) and 2 μM thapsigargin (10min) in Ca^{2+} free solution before addition of 1

mM Ca^{2+} (black bar). DPB levels are as indicated. Ca^{2+} imaging responses are means ± SEM of multiple cells per field, typical of at least 3 independent experiments.

Fig. S2. Comparative reversibility of effects of DPB162 and 2-APB STIM1/Orai-mediated Ca^{2+} entry. Fura-2 responses were in HEK-STIM1-Orai1 cells in Ca^{2+}-free medium with either DMSO (A), 2 μM DPB162 (B) or 50 μM 2-APB (C) added 10 min prior to t=0. Ca^{2+} stores were depleted with 2 μM TG, 10 min prior to experiment. Ca^{2+} free medium was maintained with two transient additions of 1 mM Ca^{2+} applied 10 min apart (bars). At the end of the first Ca^{2+} addition, washout of DMSO, DPB162 or 2-APB was commenced. Cells were subsequently maintained without DMSO or DPB162 or 2-APB. (D) Normalized average second peak from (A-C). DPB (B) or 2-APB (C) treated groups were normalized against the DMSO group (A). Results are means ± SEM of multiple cells per field and results are typical of at least 3 independent experiments. ***, $p<0.001$; unpaired Student's t test.

Fig. S3. DPB162 does not inhibit the physical coupling between STIM1 and Orai1. In HEK cells stably expressing Orai1-CFP and STIM1-YFP, were treated with 2 μM TG (arrow). Store depletion-induced change in FRET ($\Delta FRET/FRET_{rest}\%$) between Orai-CFP and STIM1-YFP are show in response to DMSO (blue) or 2 μM DPB162 (red), and 50 μM 2-APB (arrow). Right panel shows the average ± SEM peak of FRET changes. FRET responses are means ± SEM of multiple cells (5-35) per field and results are typical of at least 3 independent experiments. $p>0.05$, unpaired Student's t-test.

Fig. S4. DPB162 has no effect on CFP-SOAR/YFP-SOAR FRET. HEK wildtype cells were co-transfected with CFP-SOAR and YFP-SOAR. Change in FRET ($\Delta FRET/FRET_{rest}\%$) between CFP-SOAR and YFP-SOAR are show in response to DMSO (blue) or 2 μM DPB162 (red) (arrow). FRET responses are means ± SEM of multiple cells (5-35) per field and results are typical of at least 3 independent experiments.

Fig. 1

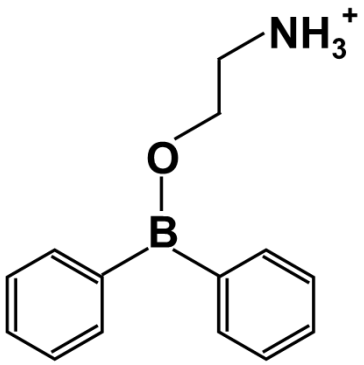

2-APB

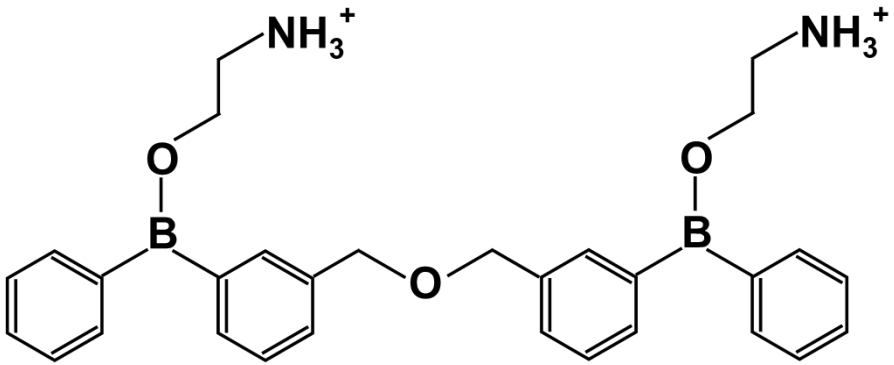

DPB162-AE

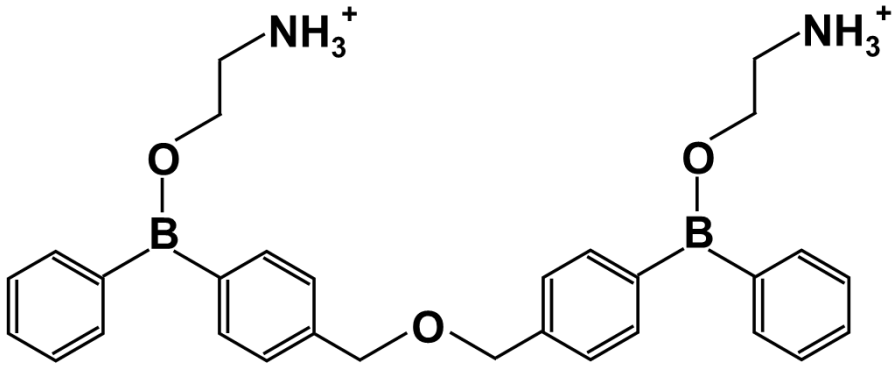

DPB163-AE

Fig. 2

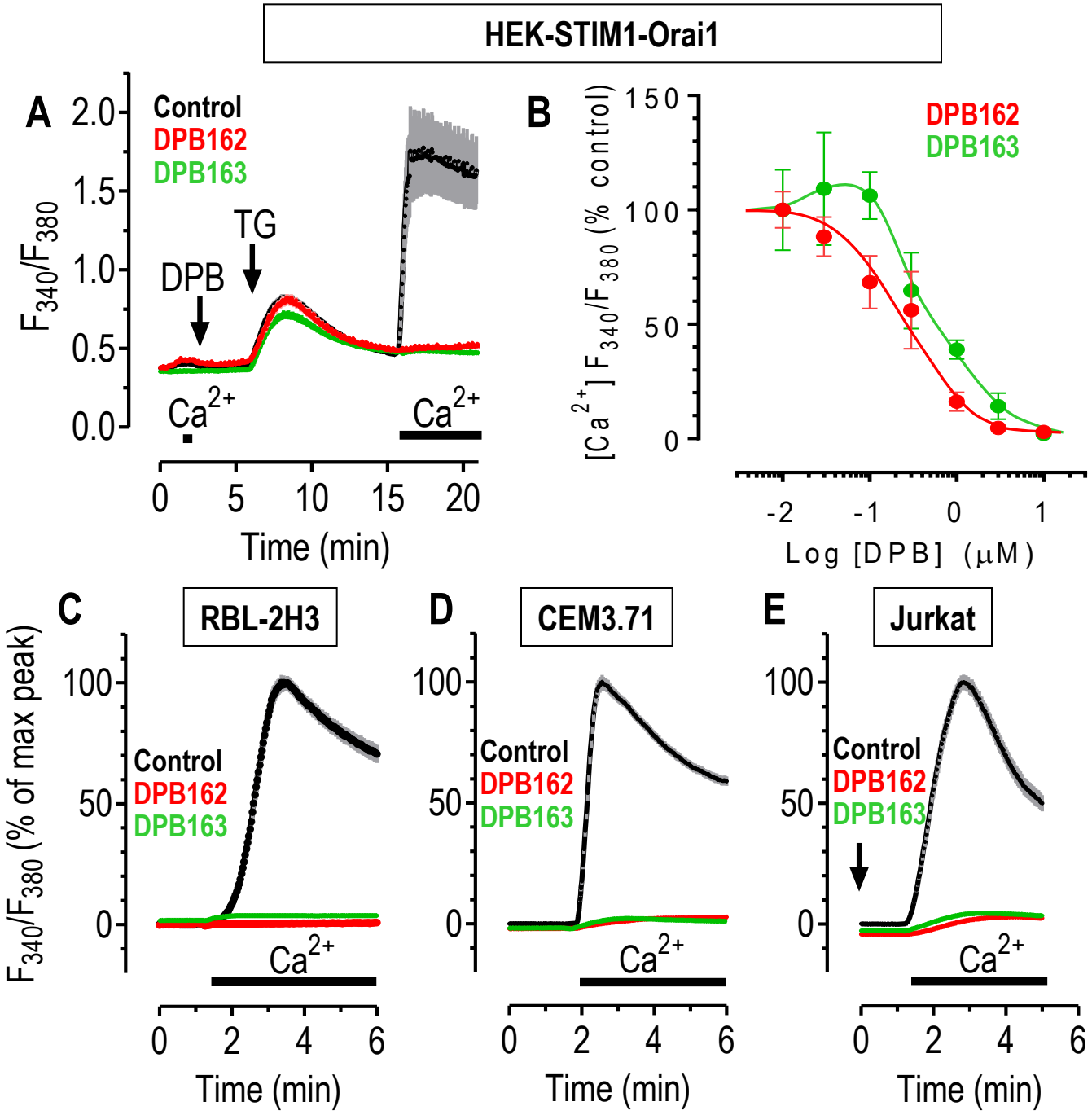
HEK-STIM1-Orai1
A
Control
DPB162
DPB163
DPB
TG
Ca2+
Ca2+
F340/F380
Time (min)
B
DPB162
DPB163
[Ca2+] F340/F380 (% control)
Log [DPB] (μM)
C
RBL-2H3
D
CEM3.71
E
Jurkat
F340/F380 (% of max peak)
Time (min)

Fig. 3

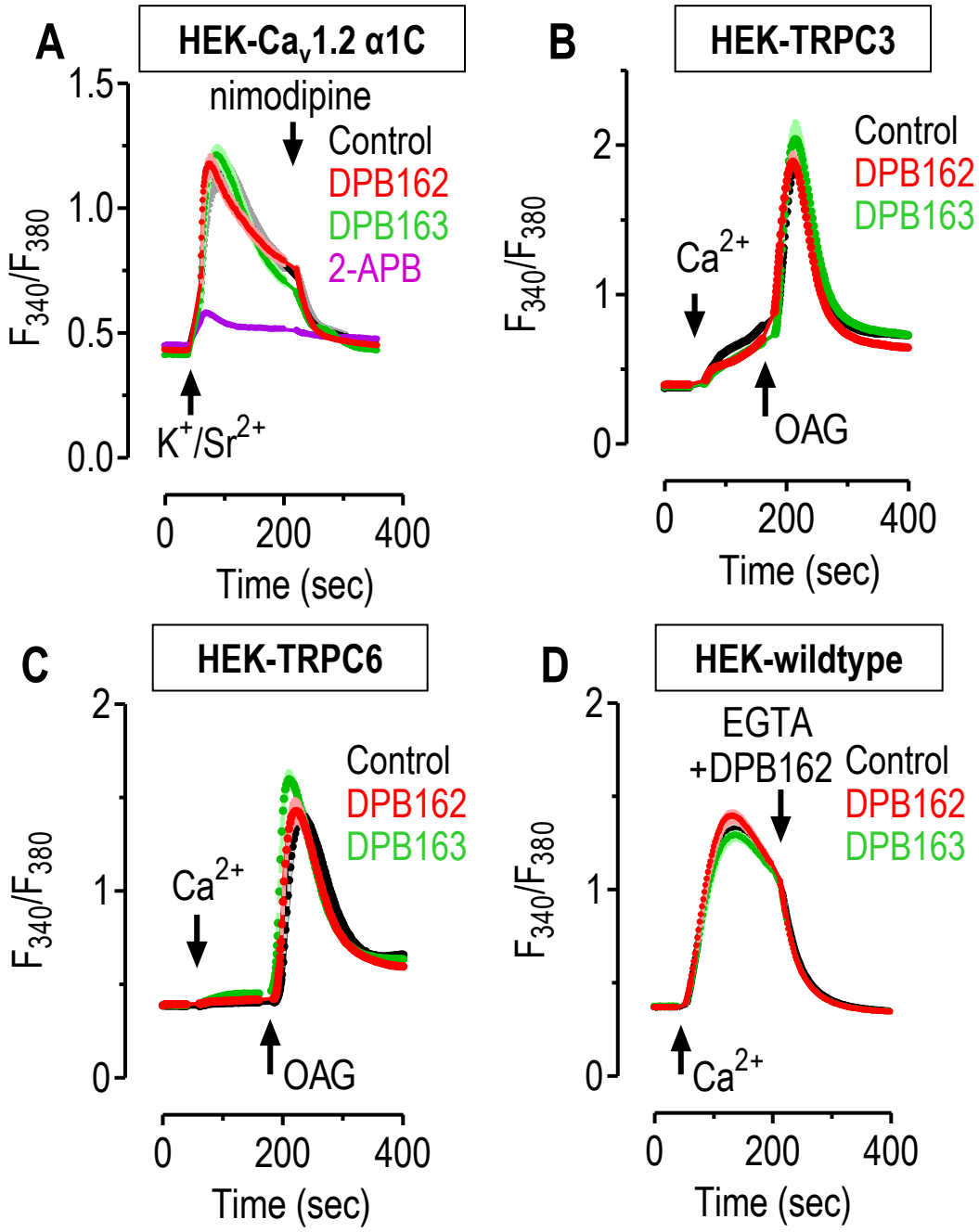
A
HEK-Cav1.2 α1C
nimodipine
Control
DPB162
DPB163
2-APB
K+/Sr2+
F340/F380
1.5
1.0
0.5
0.0
0
200
400
Time (sec)
B
HEK-TRPC3
Control
DPB162
DPB163
Ca2+
OAG
F340/F380
2
1
0
0
200
400
Time (sec)
C
HEK-TRPC6
Control
DPB162
DPB163
Ca2+
OAG
F340/F380
2
1
0
0
200
400
Time (sec)
D
HEK-wildtype
EGTA
+DPB162
Control
DPB162
DPB163
Ca2+
F340/F380
2
1
0
0
200
400
Time (sec)

Fig. 4

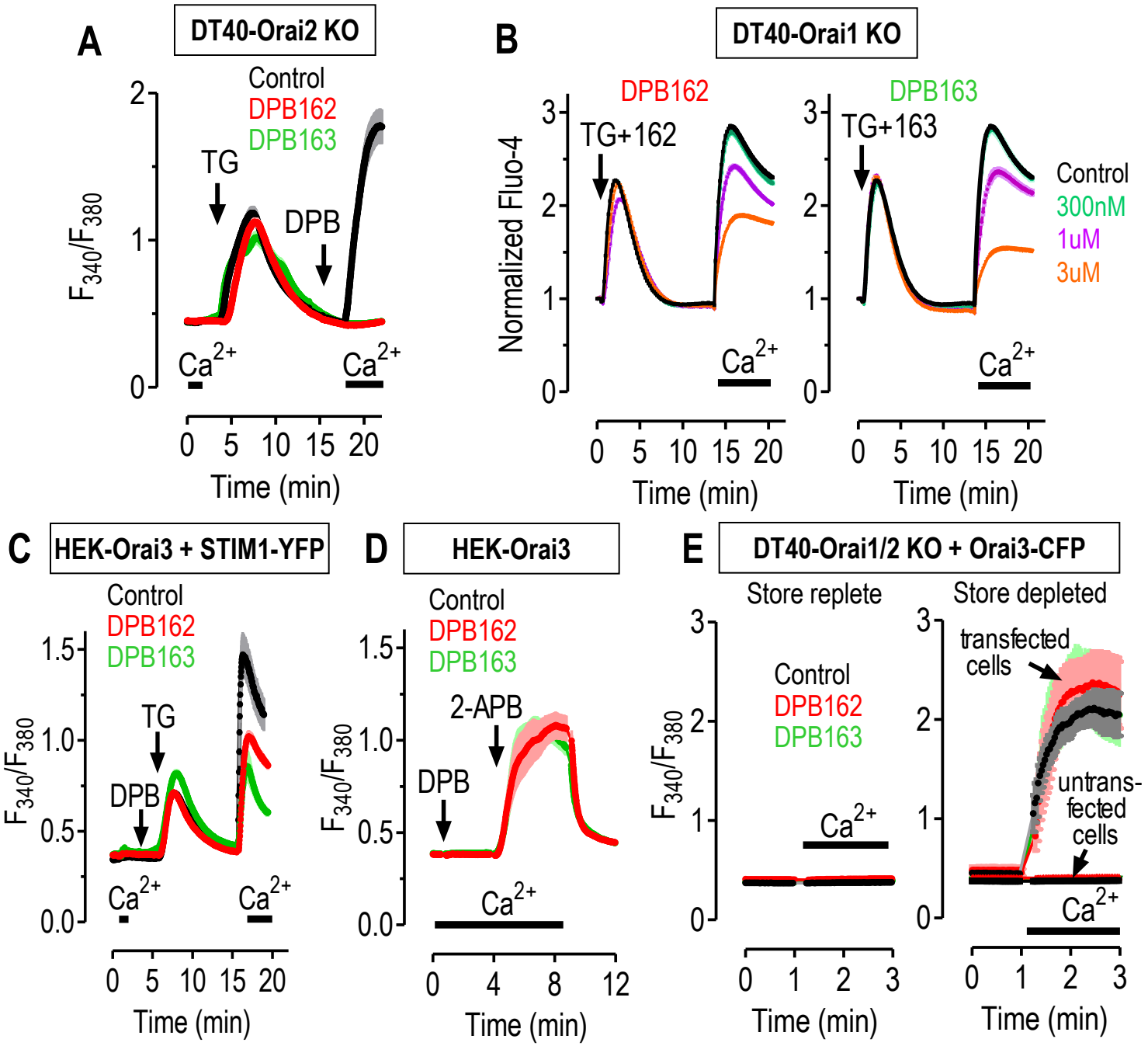
A
DT40-Orai2 KO
Control
DPB162
DPB163
TG
DPB
F_{340}/F_{380}
Ca^{2+}
Ca^{2+}
Time (min)
B
DT40-Orai1 KO
DPB162
DPB163
TG+162
TG+163
Normalized Fluo-4
Control
300nM
1uM
3uM
Ca^{2+}
Ca^{2+}
Time (min)
Time (min)
C
HEK-Orai3 + STIM1-YFP
Control
DPB162
DPB163
TG
DPB
F_{340}/F_{380}
Ca^{2+}
Ca^{2+}
Time (min)
D
HEK-Orai3
Control
DPB162
DPB163
2-APB
DPB
F_{340}/F_{380}
Ca^{2+}
Time (min)
E
DT40-Orai1/2 KO + Orai3-CFP
Store replete
Store depleted
Control
DPB162
DPB163
transfected cells
untrans-fected cells
F_{340}/F_{380}
Ca^{2+}
Ca^{2+}
Time (min)
Time (min)

Fig. 5

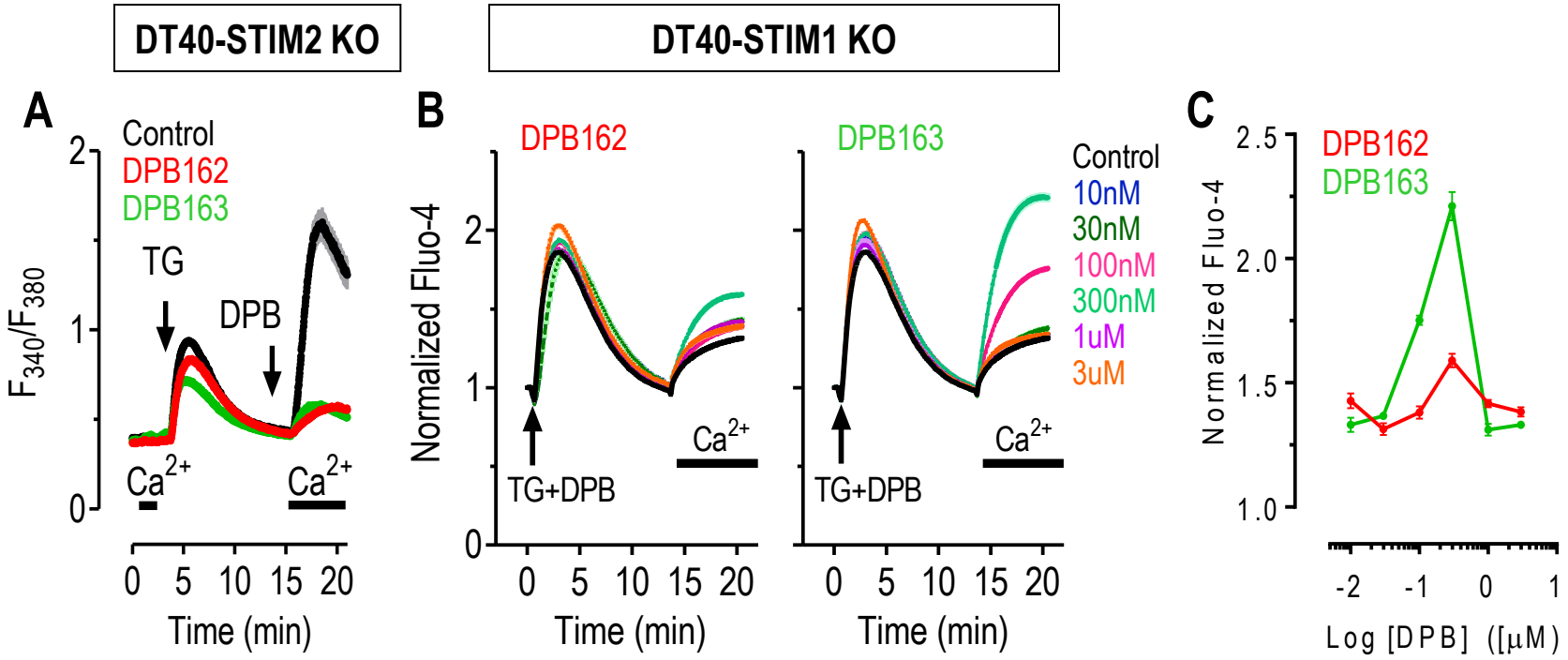
DT40-STIM2 KO
DT40-STIM1 KO
A
B
C
Control
DPB162
DPB163
TG
DPB
Ca2+
Ca2+
F340/F380
Time (min)
DPB162
DPB163
TG+DPB
TG+DPB
Ca2+
Ca2+
Normalized Fluo-4
Control
10nM
30nM
100nM
300nM
1uM
3uM
Normalized Fluo-4
Log [DPB] ([μM])

Fig. 6

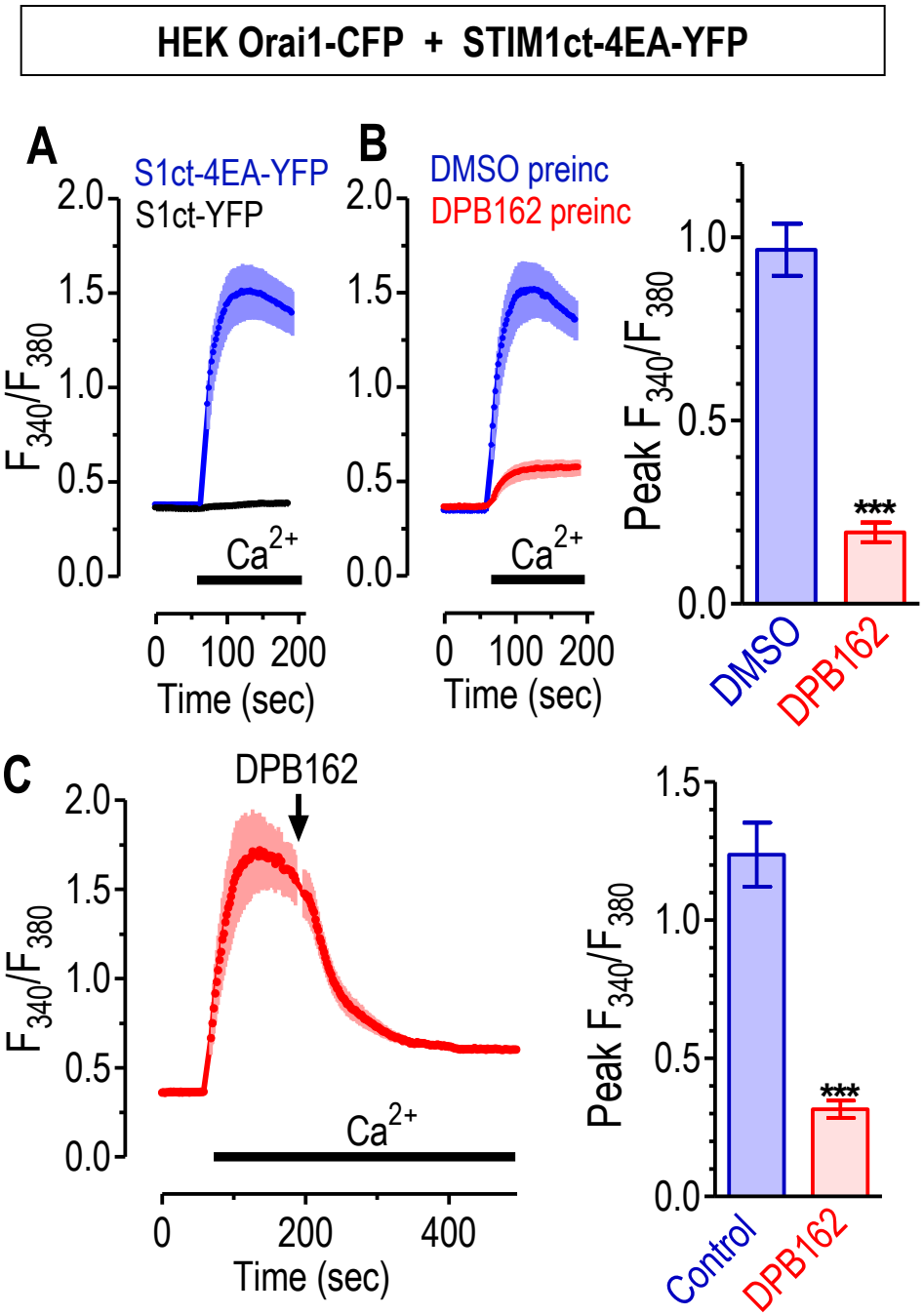
HEK Orai1-CFP + STIM1ct-4EA-YFP
A
S1ct-4EA-YFP
S1ct-YFP
F340/F380
Ca2+
Time (sec)
B
DMSO preinc
DPB162 preinc
Peak F340/F380
***
DMSO
DPB162
C
DPB162
Control
DPB162

Fig. 7

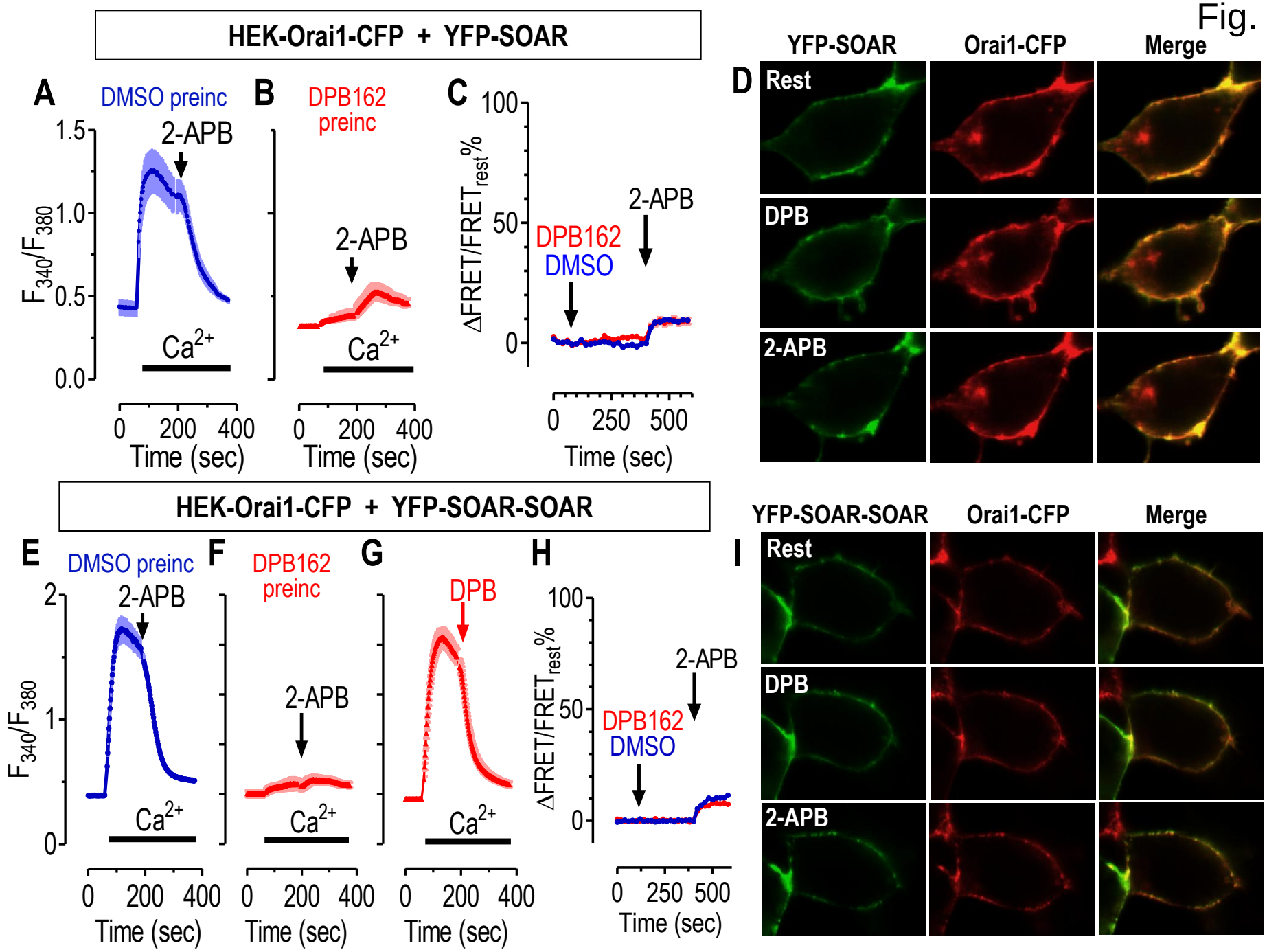
HEK-Orai1-CFP + YFP-SOAR
A
DMSO preinc
2-APB
Ca2+
B
DPB162 preinc
2-APB
Ca2+
C
DPB162
DMSO
2-APB
ΔFRET/FRETrest%
Time (sec)
D
YFP-SOAR
Orai1-CFP
Merge
Rest
DPB
2-APB
HEK-Orai1-CFP + YFP-SOAR-SOAR
E
DMSO preinc
2-APB
Ca2+
F
DPB162 preinc
2-APB
Ca2+
G
DPB
Ca2+
H
DPB162
DMSO
2-APB
ΔFRET/FRETrest%
Time (sec)
I
YFP-SOAR-SOAR
Orai1-CFP
Merge
Rest
DPB
2-APB

Fig. 8

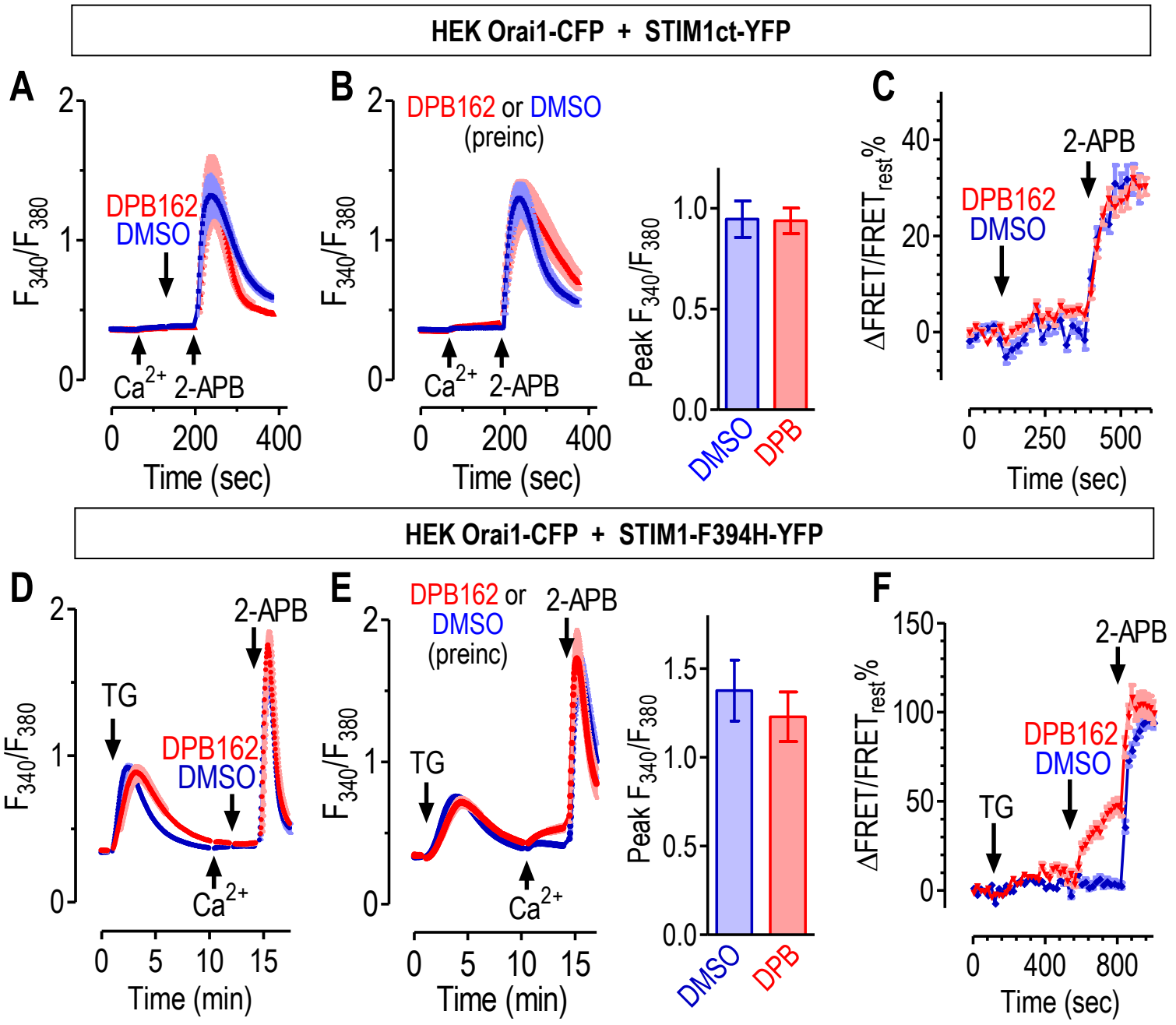
HEK Orai1-CFP + STIM1ct-YFP
A
B
C
DPB162
DMSO
DPB162 or DMSO
(preinc)
2-APB
Ca2+
F340/F380
Time (sec)
Peak F340/F380
DMSO
DPB
ΔFRET/FRETrest%
HEK Orai1-CFP + STIM1-F394H-YFP
D
E
F
TG
Time (min)

Fig. 9

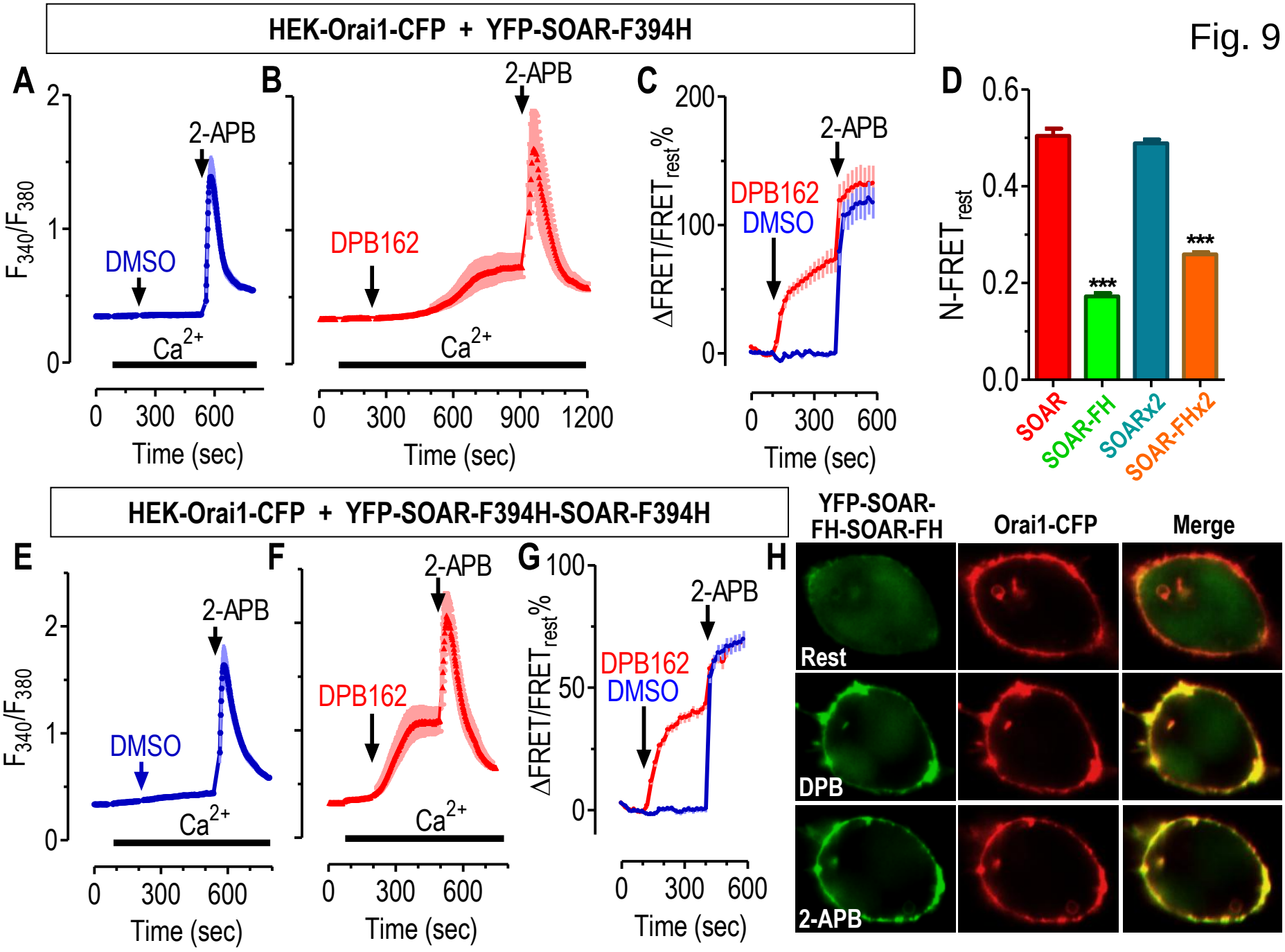
HEK-Orai1-CFP + YFP-SOAR-F394H
A
B
C
D
2-APB
DMSO
DPB162
Ca2+
F340/F380
ΔFRET/FRETrest%
N-FRET rest
Time (sec)
SOAR
SOAR-FH
SOARx2
SOAR-FHx2
***
HEK-Orai1-CFP + YFP-SOAR-F394H-SOAR-F394H
E
F
G
H
YFP-SOAR-FH-SOAR-FH
Orai1-CFP
Merge
Rest
DPB
2-APB